

European Journal of Forest Research

Combining canopy height and tree species map information for large scale timber volume estimations under strong heterogeneity of auxiliary data and variable sample plot sizes

--Manuscript Draft--

Manuscript Number:	EFOR-D-17-00182
Full Title:	Combining canopy height and tree species map information for large scale timber volume estimations under strong heterogeneity of auxiliary data and variable sample plot sizes
Article Type:	Original Research Paper
Keywords:	OLS Regression; standing timber volume; LiDAR canopy height model; satellite-based tree species classification; calibration; forest inventory; angle count sampling
Corresponding Author:	Andreas Hill Eidgenössische Technische Hochschule Zurich Zurich, SWITZERLAND
Corresponding Author Secondary Information:	
Corresponding Author's Institution:	Eidgenössische Technische Hochschule Zurich
Corresponding Author's Secondary Institution:	
First Author:	Andreas Hill, Msc.
First Author Secondary Information:	
Order of Authors:	Andreas Hill, Msc. Henning Buddenbaum, Dr. Daniel Mandallaz, Dr. habil.
Order of Authors Secondary Information:	
Funding Information:	
Abstract:	A timber-volume regression model applicable to the entire forest area of the federal German state of Rhineland-Palatinate is identified using a combination of airborne laser scanning (LiDAR)-derived metrics and information from a satellite-based tree species classification map available on the federal state level. As is common in many forest inventory datasets, strong heterogeneity in the LiDAR data due to different acquisition dates and misclassifications in the tree species classification map had noticeable effects on the regression model's performance. This article specifically addresses techniques that improve the performance of ordinary least square regression models under such restricting conditions. We introduce a calibration technique to neutralize the effect of misclassifications in the tree species variable that originally caused a residual inflation of 5%. Incorporating the calibrated tree species information improved the model accuracy by 6% in adjusted R ² and suggests the use of such information in forthcoming inventories. We also found that including LiDAR quality information as categorical variables within the regression model considerably mitigates issues with time lags between the LiDAR and terrestrial data acquisition and LiDAR quality variations (9% increase in adjusted R ²). The model achieved an adjusted R ² of 0.49 (RMSE cv of 132 m ³ /ha) under incorporation of the tree species and LiDAR quality information, and was thus improved by 14% (16 m ³ /ha) compared to the simple model only containing LiDAR height metrics (adjusted R ² =0.35, RMSE cv =148 m ³ /ha).
Suggested Reviewers:	Johannes Breidenbach, Dr. Research Professor, Norwegian Institute of Bioeconomy Research johannes.breidenbach@nibio.no Johannes Breidenbach has gained international reputation in the field of model

	<p>dependent and model assisted forest inventory applications. His particular focus has been on processing remote sensing information for subsequent integration in prediction models that are used in existing forest inventories. Having contributed to forest inventory methods applied in Canada, the United States, Germany and Norway, we consider Mr. Breidenbach as an excellent reviewer to assess the contribution of our article in an international context.</p>
	<p>Steen Magnussen, Dr. Research Scientist, Pacific Forestry Centre steen.magnussen@canada.ca</p> <p>Steen Magnussen is an internationally recognized expert in the field of statistics, multiresource forest inventories, and classification and accuracy of forest inventory information. He has specifically addressed the potential effects of error-prone explanatory variables on regression models in the frame of model-supported forest inventories in one of his publications. We thus consider him to be an excellent reviewer with respect to all aspects of our article.</p>
	<p>Hollaus Markus, Dr. Senior Scientist, Technische Universität Wien Markus.Hollaus@geo.tuwien.ac.at</p> <p>Markus Hollaus is an internationally recognized expert in processing LiDAR data for timber volume modeling in the frame of small-scale and large-scale forest inventories. He has specifically addressed the challenges of deriving LiDAR explanatory variables under variable sample plot sizes, i.e. angle count sampling, in his publications. We thus consider him to be an excellent reviewer.</p>
	<p>Gerald Kändler, Dr. Head of Department, Federal Forest Research Institute Baden-Württemberg gerald.kaendler@forst.bwl.de</p> <p>Gerald Kändler is head of the Biometrics and Informatics Department of the federal forest research institute Baden-Württemberg and specialized on biometrics and forest inventories. He is co-developer of the taper models and inventory methods applied in the German National Forest Inventory. His research focusses on extending existing forest inventories to double-sampling procedures. We thus consider him to provide valuable contributions as reviewer to our article.</p>

European Journal of Forest Research manuscript No.
(will be inserted by the editor)

Combining canopy height and tree species map information for large scale timber volume estimations under strong heterogeneity of auxiliary data and variable sample plot sizes

Andreas Hill · Henning Buddenbaum · Daniel Mandallaz

Received: date / Accepted: date

Abstract A timber-volume regression model applicable to the entire forest area of the federal German state of Rhineland-Palatinate is identified using a combination of airborne laser scanning (LiDAR)-derived metrics and information from a satellite-based tree species classification map available on the federal state level. As is common in many forest inventory datasets, strong heterogeneity in the LiDAR data due to different acquisition dates and misclassifications in the tree species classification map had noticeable effects on the regression model's performance. This article specifically addresses techniques that improve the performance of ordinary least square regression models under such restricting conditions. We introduce a calibration technique to neutralize the effect of misclassifications in the tree species variable that originally caused a residual inflation of 5%. Incorporating the calibrated tree species information improved the model accuracy by 6% in adjusted R^2 and suggests the use of such information in forthcoming inventories. We also found that including LiDAR quality information as categorical variables within the regression model considerably mitigates issues with time lags between the LiDAR and terrestrial data acquisition and LiDAR quality variations (9% in-

crease in adjusted R^2). The model achieved an adjusted R^2 of 0.49 (RMSE_{cv} of 132 m³/ha) under incorporation of the tree species and LiDAR quality information, and was thus improved by 14% (16 m³/ha) compared to the simple model only containing LiDAR height metrics (adjusted R^2 =0.35, RMSE_{cv}=148 m³/ha).

Keywords OLS Regression · standing timber volume · LiDAR canopy height model · satellite-based tree species classification · calibration · forest inventory · angle count sampling

1 Introduction

Forest inventory methods are the primary tools used to assess the current state and development of forests over time. They provide reliable evidence-based information that is used to define and identify management actions as well as to adapt forest management strategies to both national and international guidelines. Two methods that have recently become particularly attractive are so-called *double-sampling* (Mandallaz, 2008) and *mapping* (Beaudoin et al, 2014) procedures. The core concept of these methods is to use predictions of the terrestrial target variable at additional sample locations where the terrestrial information has not been gathered. These predictions are produced by models that use explanatory variables derived from *auxiliary data*, commonly in the form of spatially exhaustive remote sensing data in the inventory area. The specific scope of double-sampling is to enlarge the terrestrial sample size by a much larger sample of predictions of the target variable in order to gain higher estimation precision without performing additional expensive terrestrial measurements. Model-based and model-assisted regression estimators are used in a broad range of double sampling concepts and methods (Gregoire and Valentine, 2007; Köhl et al, 2006; Mandallaz, 2013a,b;

Andreas Hill
Department of Environmental Systems Science, ETH Zurich, Universitaetstrasse 22, 8092 Zurich, Switzerland
Tel.: +41 44 632 32 36
E-mail: andreas.hill@usys.ethz.ch

Henning Buddenbaum
Environmental Remote Sensing and Geoinformatics Department, Trier University, 54286 Trier, Germany
Tel.: +49 651 201 4729
E-mail: buddenbaum@uni-trier.de

Daniel Mandallaz
Department of Environmental Systems Science, ETH Zurich, Universitaetstrasse 22, 8092 Zurich, Switzerland
Tel.: +41 44 632 88 35
E-mail: daniel.mandallaz@usys.ethz.ch

Saborowski et al., 2010; Schreuder et al., 1993) and have been applied to existing inventory systems (Breidenbach and Astrup, 2012; von Lüpke and Saborowski, 2014; Magnussen et al., 2014; Mandallaz et al., 2013; Massey et al., 2014). While double-sampling methods provide reliable estimates for a given spatial unit, e.g. a forest district, they do not provide information about the spatial distribution of the estimated quantity within this area. For this reason, the same modeling technique used in double-sampling procedures has also been intensively used to produce exhaustive prediction maps that provide pixelwise estimations of a target variable in high spatial resolution (Hill et al., 2014; Latifi et al., 2010; Nink et al., 2015; Tonolli et al., 2011; Van Aardt et al., 2008).

To allow for an area-wide application of the prediction model, both double sampling and mapping methods require that the remote sensing data are available over the entire inventory area. This is usually not a limiting factor in *small-scale* applications. In the optimal case, the remote sensing data are in principle collected in accordance to the specific study objective. Quality standards that have often been addressed are that *a)* the remote sensing data should be acquired close to or even at the time of the terrestrial inventory in order to ensure best possible comparability between the target variable on the ground and the remote sensing derived variables (McRoberts et al., 2015); *b)* the remote sensing technology and its spectral and spatial resolution should be chosen according to the modelling purpose (Köhl et al., 2006); and *c)* the variation in quality of the remote sensing data over the inventory area should be minimized in order to avoid artificial noise in the data (Naesset, 2014). Despite the increasing availability and decreasing costs of remote sensing data (White et al., 2016), these quality standards of the remote sensing data can often not be guaranteed for *large-scale* applications (Maack et al., 2016), and trade-offs must be accepted (Jakubowski et al., 2013). The prime objective is then to produce the best possible prediction model given the restrictions imposed by the available remote sensing information. The exploration of scarcely used remote sensing products and the optimization of prediction models under severe quality restrictions in the remote sensing data are thus one of the challenges in large-scale model-supported inventory applications.

Among the still rarely used remote sensing data in large scale applications, the use of tree species information in prediction models - especially for timber volume estimation - has been stated as some of the most promising but often missing information (Koch, 2010; White et al., 2016). As timber volume estimations on the single tree level in forest inventories are often based on species-specific biomass and volume equations (Husmann et al., 2017; Zianis et al., 2005), the application of species-specific models is expected to be a key factor for improving estimation precision (White et al., 2016). Straub et al. (2009) and Latifi et al. (2012) reported

a notable gain in model performances when using stratification according to broadleaf and coniferous tree species on sample plot level in conjugation to canopy height metrics for timber volume estimations. One of the rare examples of using more species-specific information is Packalén and Maltamo (2006), who applied a separate prediction of the sample plot timber volume for Scots pine, Norway spruce and a deciduous-species group. However, further investigation is necessary especially in countries whose forests are characterized by a larger variety of tree species that may also occur in mixed and uneven-aged stands (McRoberts et al., 2010). The area-wide tree species information in most studies was obtained from satellite and airborne remote sensing sensors based on automatic classification methods. Whereas the presence of misclassifications has already been addressed (Latifi et al., 2012), an issue that has so far been neglected is how misclassifications actually affect the prediction model (Gustafson, 2003).

A frequently encountered problem in large scale forest inventories is the lack of temporal synchronicity between the remote sensing acquisition and the terrestrial survey. As a result, the available remote sensing data often exhibit notable time-lags with respect to the date of the terrestrial inventory. This has often been addressed as a major drawback, especially for the application of model-assisted change estimation (Massey and Mandallaz, 2015).

Our study is embedded in the current implementation of model-assisted regression estimators (Mandallaz, 2013a,b; Mandallaz et al., 2013) for estimating the standing timber volume within the state and communal forest management units over the entire state of Rhineland-Palatinate (RLP, Germany). With respect to this overall objective, the aim of this study was to derive an ordinary least square (OLS) regression model to generate predictions of the standing timber volume associated with a sample location of the Third German National Forest Inventory (BWI3) over the entire federal state forest area (6155 km^2). A merged LiDAR dataset from different acquisition years and a satellite-based tree species classification map for the five main tree species in RLP was available for the entire inventory area and consequently used to derive predictor variables. The major limiting factors for using these data in a regression analysis are **(i)** variation in the LiDAR data quality as well as time-lags of up to 10 years between the LiDAR acquisitions and the terrestrial survey, **(ii)** misclassifications in the tree species classification map and **(iii)** the ambiguous choice of a suitable extraction area (*support*) for all remote sensing information under angle count sampling in the terrestrial survey (variable sample plot sizes). For this reason, we address the following specific research questions:

1. How can tree species map information be optimally used within a regression model that predicts timber volume?

- 1 What effects do misclassifications have on the predictions and how can these effects be minimized?
 2
 3
 4
 5
 6
 7
 8
 9
 10
 11
 12
 13
 14
 15
 16
 17
 18
 19
 20
 21
 22
 23
 24
 25
 26
 27
 28
 29
 30
 31
 32
 33
 34
 35
 36
 37
 38
 39
 40
 41
 42
 43
 44
 45
 46
 47
 48
 49
 50
 51
 52
 53
 54
 55
 56
 57
 58
 59
 60
 61
 62
 63
 64
 65
1. What effects do misclassifications have on the predictions and how can these effects be minimized?
 2. What are the effects of quality restrictions and substantial time lags between the LiDAR- and terrestrial data acquisition on the regression model and how can these effects be mitigated?
 3. Does support size influence model accuracy? What is the optimal support size and what are the determining factors?

2 Materials and Methods

2.1 Study Area

The German federal state Rhineland-Palatinate (RLP) is located in the western part of Germany and borders Luxembourg, France and Belgium (figure 1). With 42.3% (appr. 8400 km²) of the entire state area (19850 km²) covered by forest, RLP is one of the two states with the highest forest coverage among all federal states of Germany (von Thünen-Institut, 2014). The most frequent tree species in RLP are European beech (*fagus sylvatica*, 21.8%), oak (*quercus petrea* and *quercus robur*, 20.2%), Norway spruce (*picea abies*, 19.5%), Scots pine (*pinus sylvestris*, 9.9%), Douglas fir (*pseudotsuga menziesii*, 6.4%), European larch (*larix decidua*, 2.4%) and Silver fir (*abies alba*, 0.7%). The share of broadleaf tree species is 58.7%. The forests of RLP further exhibit heterogeneous structures (von Thünen-Institut, 2014): around 82% of the forest area in RLP are mixed forest stands (i.e. at least two different tree species occur in the same stand) and 69% of the forest area exhibit a multi-layered vertical structure. While the average tree age is around 80 years, most of the forest area (20%) is occupied by trees between 40 and 60 years of age, whereas 27% of the trees are older than 100 years. Spatially variable climate conditions have a strong influence on the local growth dynamics as well as tree species composition and create a large variety of forest structures, ranging from characteristic oak coppices (Moselle valley), pure spruce, beech and scots pine forests (e.g. Hunsrück and Palatinate forest) to mixed forests comprising variable proportions of oak, larch, spruce, Scots pine and beech. Accordingly, RLP has been divided into 16 bioclimatic growing regions that form homogeneous areas with respect to the afore mentioned characteristics (Gauer and Aldinger, 2005).

2.2 Terrestrial Inventory Data

The German National Forest Inventory is carried out over the entire forest area of Germany in reoccurring time periods of 10 years. The most recent inventory (BWI3) has been conducted in the years 2011 and 2012. In this framework,

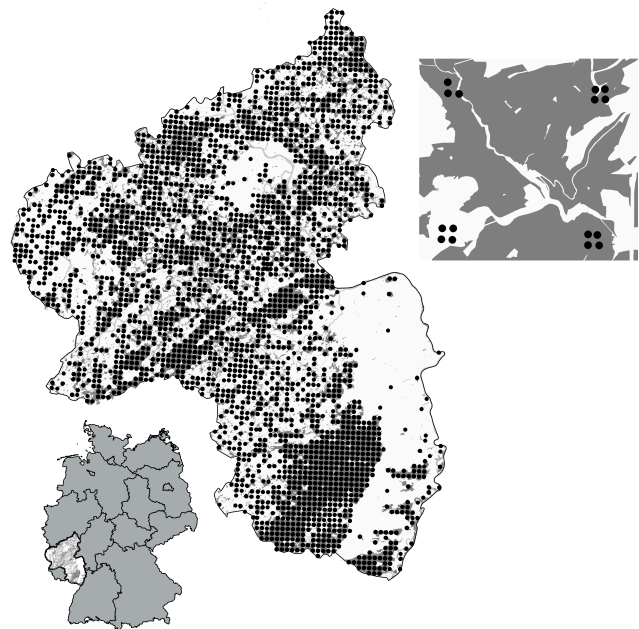


Fig. 1: Spatial distribution of the BWI3 cluster samples over Rhineland-Palatinate

Rhineland-Palatinate is covered by a 2x2 km grid that defines the sample locations for the terrestrial survey. A sample unit consists of four sample locations (also referred to as *sample plots*) that are arranged in squares (so called *clusters*) with a side length of 150 metres (figure 1). The number of plots per cluster can however vary between 1 and 4 depending on forest/non-forest decisions on the plot level (Bundesministerium für Ernährung, 2011). In the field survey of the BWI3, sample trees for timber volume estimations are selected according to the angle count sampling technique (Bitterlich, 1984), using a basal area factor (*BAF*) of 4 that is respectively adjusted for boundary effects at the forest border (Bundesministerium für Ernährung, 2011). A further selection criterion for a tree to be recorded is a diameter at breast height (*dbh*) of at least 7 cm. This sampling technique was applied to 8092 sample plots (2810 clusters) in RLP, resulting in the collection of 56561 sample trees for which the *dbh*, the absolute tree height, the tree diameter at 7 m (*D7*) and the tree species were recorded. All plot center positions were determined with a differential GPS technique. In order to derive a volume estimation for each sample tree, the BWI3 estimates a taper curve for each sample tree by calibrating the random effects term of linear mixed-effects taper models with the set of diameters and corresponding height measurements taken from the respective sample tree (Kublin et al, 2013). The integration of the derived taper curves consequently lead to a volume prediction for each sample tree. We restricted the sampling frame exclusively to the area of state and communal forest management units, which constitute 73% of the entire forest area of RLP (von Thünen-

[Institut, 2014](#)). The dataset of this study hence comprised 5791 plots (2055 clusters). For this sample, the timber volume density per hectare on plot level, $Y(x)$, was calculated according to the formula of one-phase one-stage sampling ([Mandallaz, 2008](#)). The timber volume density per hectare on plot level was used as the response variable in the regression analysis.

10 2.3 Auxiliary Information

11 12 13 2.3.1 LiDAR Canopy Height Model

14 Between 2003 and 2013, the topographic survey institution
 15 of RLP acquired airborne laser scanning (LiDAR) data
 16 over the entire state of RLP at leaf-off condition (Figure
 17 [2](#)). The objective of this campaign was to derive a coun-
 18 trywide digital terrain and surface model based on the ac-
 19 quired LiDAR point clouds. During the extended acquisi-
 20 tion period, airborne laser scanning technology and data
 21 quality evolved significantly. The tiles recorded in 2002 and
 22 2003 have a rather poor quality with about only 1 point per
 23 $5 \times 5 \text{ m}^2$, while more recently acquired datasets contain more
 24 than 125 points per $5 \times 5 \text{ m}^2$ raster cell. The data was deliv-
 25 ered as two separate point clouds: one cloud contained fil-
 26 tered ground returns, whereas the other cloud contained first
 27 pulses from non-ground objects. All point clouds were de-
 28 livered as three-column (easting, northing, and height above
 29 sea level) ASCII files in tiles of 1 km^2 . Before interpo-
 30 lating the point clouds to regular rasters, the clouds were
 31 thinned. For the ground data, the mean value of each raster
 32 cell in the final resolution of $5 \times 5 \text{ m}^2$ was calculated. For
 33 the surface model, both ground and vegetation point clouds
 34 were first united, and the maximum value for each raster
 35 cell was determined respectively. The combination of both
 36 point clouds was necessary in order to avoid large spaces
 37 without laser points between vegetated areas that would oth-
 38 erwise have been filled with unrealistic values in the inter-
 39 polation step. The thinned point clouds were aggregated to
 40 larger tiles in order to decrease the number of seamlines
 41 in the final mosaic. The aggregated tiles were then interpo-
 42 lated to raster images using a Delaunay interpolation in the
 43 Matlab software ([Mathworks, 2017](#)). The resulting two ele-
 44 vation models were then used to calculate a canopy height
 45 model (CHM) in raster format, providing discrete informa-
 46 tion about the canopy surface height of the forest area in a
 47 spatial resolution of 5 meters.

52 As explanatory variables, the mean canopy height
 53 (*meanheight*) and the standard deviation (*stddev*) were cal-
 54 culated as the mean and standard deviation of all raster val-
 55 ues within a predefined square around each sample plot cen-
 56 ter. The square (i.e. *support* of the explanatory variable,
 57 see section [2.4](#)) was previously intersected with the state
 58 and communal forest area defined by a polygon mask and

59 thereby corrected for edge effects at the forest border. The
 60 tree height is one prominent predictor variable in the taper
 61 functions of the BWI3 that are used to calculate a timber vol-
 62 ume value for each sample tree ([Kublin, 2003; Kublin et al,](#)
 63 [2013](#)). A visual inspection of the tree volumes of all sample
 64 trees collected in the BWI3 within RLP against their tree
 65 heights also revealed the characteristic shape of an allome-
 66 tric relationship between these variables (Online Resource
 67 1). It was hypothesized that this relationship on single-tree
 68 level is also apparent on the aggregated level of a sample plot
 69 and cluster, and can be used within the frame of regression
 70 modeling.

71 The strength of correlation between *meanheight* and
 72 timber volume on plot level was expected to show high vari-
 73 ation according to the mentioned time-lag up to 10 years
 74 between LiDAR acquisition and terrestrial survey. The qual-
 75 ity of the height information was also expected to vary acc-
 76 cording to changing sensor technologies and different point
 77 densities used over the years. For these reasons, the LiDAR
 78 acquisition year (*lidaryear*) for each sample plot was con-
 79 sidered as a potential categorical explanatory variable to ex-
 80 plain the variation in the data introduced by these factors.
 81 For this purpose, the acquisition year *2008* was further di-
 82 vided into *2008* and *2008_1*. In the latter, the data quality
 83 turned out to be very poor due to sensor failures during
 84 the acquisition. Additionally, the years *2006* and *2007* as
 85 well as *2012* and *2013* were pooled in order to increase the
 86 number of observations per factor level for modelling rea-
 87 sons. As a result, the *lidaryear* variable comprised nine cat-
 88 egories (*2002, 2003, 2007, 2008, 2008_1, 2009, 2010, 2011*
 89 and *2012*).

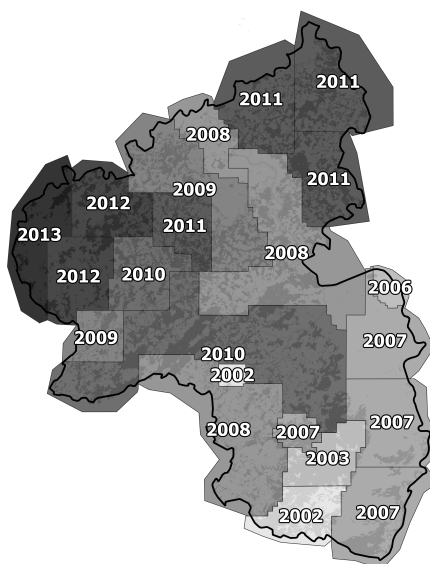


Fig. 2: Separate LiDAR acquisitions in Rhineland-Palatinate over the years. The colors also indicate the quality of the data: *light*: low point densities ($1/5 \times 5 \text{ m}^2$), *dark*: high point densities ($>100/5 \times 5 \text{ m}^2$)

2.3.2 Tree Species Classification Map

A countrywide satellite-based classification map of the five main tree species (European beech, Sessile and Pedunculate oak, Norway spruce, Douglas fir, Scots pine) described in Stoffels et al (2015) was used to derive tree species information on sample plot level. The classified tree species map has a grid size of 5 meters and predicts five of the seven tree species that are used in the BWI3 taper functions (Kublin et al, 2013) to calculate the timber volume of a sample tree. Due to unavailable satellite data for the classification, the tree species map excluded one patch with an area of 415 km² in the south-west part of RLP, and two further patches with an area of 76 km² and 100 km² in the northern part (Stoffels et al, 2015). The tree species information was consequently missing for 407 (7%) of the 5791 sample locations.

Prediction of main plot tree species

A visual inspection of all BWI3 sample trees of RLP suggested that a stratification of the relation between tree height and timber volume according to these seven tree species may provide a considerable reduction in variation within the tree species groups (Online Resource 1). This led to the hypothesis that this tree species specific signal might also be apparent on sample plot and cluster level and can consequently be used to increase the accuracy of the prediction model. Based on the tree species classification map, the main tree species of each sample plot was calculated as an additional categorical explanatory variable (*treespecies*) with six categories following a similar approach as Latifi et al (2012): one of the five tree species was assigned as the main plot tree species if its proportion within the edge-corrected support around the sample location exceeded a predefined threshold. If this threshold was not reached by any of the five tree species, the respective sample plot was assigned the category 'Mixed'.

Calibration

Our analyses revealed that the prediction of the main tree species for a sample plot can be subject to misclassifications (section 3.1). Errors in the explanatory variables of linear regression models can however lead to a bias of the regression coefficients in the direction of zero due to an artificial introduction of noise (Carroll et al, 2006). This can cause an inflation of the residual variance and a consequent decrease of the model accuracy (Magnussen et al, 2010). In case of classification the impacts of misclassifications on the model properties are even harder to predict (Gustafson, 2003). While errors in the explanatory variables do not affect the unbiasedness of the estimators in the model-assisted framework, a reduction or elimination of the classification errors could provide an improvement of the regression model accuracy and thereby potentially lead to smaller prediction and

estimation errors. We therefore addressed the effect of misclassifications in the *treespecies* variable by the following analysis:

- a) we investigated the effect on the regression model performance (regression coefficients, model accuracy) when substituting the *predicted* by the *actual* main plot tree species derived from the sampled trees of the respective sample plot under identical threshold settings
- b) we used the random forest algorithm (Breiman, 2001; Liaw and Wiener, 2002) in the statistical software R (R Core Team, 2016) to define a *calibration model* in order to improve the classification accuracy of the initially predicted main plot tree species, correct for potential systematic misclassifications and thus minimize the effect of misclassifications on the regression model. The random forest algorithm is a machine learning algorithm that grows a large number of decorrelated classification trees by considering only a subset of all provided predictor variables for each split. In the case of classification, new data are thus predicted by aggregating the predictions of all trees using a majority vote. For our purpose of predicting the actual main tree species of a sample plot (target variable), we provided the random forest algorithm with a full set of p predictor variables that comprised the initial prediction of the main plot tree species (*treespecies*), the mean canopy height (*meanheight*) and standard deviation (*stddev*) derived from the CHM, the proportion of coniferous trees estimated from the tree species classification map (*prop.conif*) and the bioclimatic growing region (*wgb*) at the sample location. The algorithm was grown with 2000 trees, considering $\sqrt{p} \approx 3$ of the predictors for each split.

2.4 Choice of Support under Angle Count Sampling

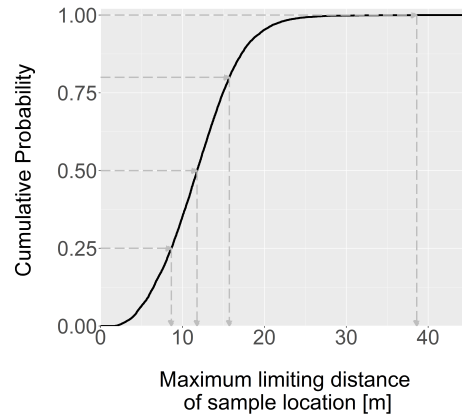
One characteristic of angle count sampling applied in the BWI3 is that a sample plot does not have a fixed radius in which trees are selected (*fixed-radius plot*), but each tree generates an individual radius from the plot center depending on its diameter at breast height (*variable-radius plot*). This tree-individual radius is known as the *limiting distance* from the plot center where the tree would still be included in the sample. A consequence of the absence of a fixed plot radius is the question about the optimal support (Hollaus et al, 2007), i.e. the spatial extent around the plot center in which the auxiliary information is evaluated and transformed into an explanatory variable. It has widely been hypothesized that the best relationship between the target variable on the ground and any explanatory variable derived from the auxiliary information is obtained if the support is spatially identical to the sample plot extent. In case of angle count sampling, an individual extent for each sample plot can be ap-

proximated by regarding the maximum limiting distances of its sample trees as the outer plot radius. However, many model-assisted applications under double-sampling do not allow for a between-plot change of the support for a specific explanatory variable (Mandalaz, 2013a,b).

For this reason, the task is to find a unique support for each auxiliary information that leads to the best overall model accuracy. Deo et al (2016) conducted extensive analysis to identify optimal supports for modelling standing timber volume for *variable-radius plot* designs in conifer forests. They analysed 24 different radii (i.e. circular supports) in which they extracted 57 metrics from a LiDAR derived point cloud with an average point density of 18 pulses per square meter. They successively evaluated the prediction performance of each support size by using the LiDAR metrics in a random forest algorithm and comparing the resulting model accuracies. In order to identify the best-performing supports for our explanatory variables, we followed a similar approach. The explanatory variables were calculated using *individual* (i.e. plot-varying) supports (*ind*), i.e. an individual support extent was used for each plot according to the maximum limiting distance of all sample trees associated to the respective sample plot. We then compared the model accuracies achieved by the individual supports against the model accuracies from a set of *fixed* (i.e. non plot-varying) supports. The extents of the fixed supports were chosen from the cumulative distribution function (ECDF) of the maximum limiting distances of all 5791 sample plots of the analysed forest area (Fig. 3a). We considered the 25th (q_{25} , 9 meters), 50th (q_{50} , 12 meters), 80th (q_{80} , 15 meters) and the 100th (q_{100} , 38 meters) percentiles, resulting in support side lengths of 18, 24, 30 and 76 meters (Fig. 3). In contrast to the approach of Deo et al (2016), the theory of the model-assisted regression estimators by Mandalaz (2013a,b) required the explanatory variables to be calculated using supports that theoretically allow for a tessellation of the entire forest area (i.e. rectangular supports). Based on the underlying theory the use of different support sizes for each explanatory variable is however perfectly valid.

45 2.5 Model Validation

In order to judge the quality of the *treespecies* variable, the user's accuracy for each classified species and the overall accuracy of the classification scheme was calculated based on the confusion matrix (Congalton and Green, 2008), using the main plot tree species calculated from the sample trees as reference data. The classification accuracy was performed for all support sizes for both the calibrated and the uncalibrated *treespecies* variables. The measures of the regression model accuracy using both CHM- and *treespecies* variables were defined as the 10-fold cross-validated root mean square error (RMSE_{cv}) and



(a) ECDF of maximum limiting distances of all BWI3 sample locations in RLP



(b) Rectangular supports used to extract explanatory variables around sample locations.
Dash dot dot line: q100, dash dot line: q80, dot dot line: q50, dot line: q25, solid line: individual support, triangles: sample trees

Fig. 3: Identification (a)) and visualization (b)) of potential supports used for calculating the predictor variables on plot level

the adjusted coefficient of determination (adjusted R^2) of the multiple linear regression model defined in equation 1. Additionally, we considered the interaction terms *meanheight:treespecies*, *meanheight²:treespecies*, *meanheight:lidaryear*, *stddev:lidaryear* and *meanheight:stddev* and performed a variable selection based on the Akaike Information Criterion (AIC) (Akaike, 2011) in order to minimize the number of variables in the model. Due to a pronounced unbalanced design in the *treespecies-lidaryear* strata (Online Resource 2), no interaction between *treespecies* and *lidaryear* was possible. We evaluated the model for all support combinations, considering the use of individual support sizes for each auxiliary information, using both the calibrated and the uncalibrated *treespecies* variable. The calibration model (section 2.3.2)

for the *treespecies* variable was recalculated for each respective support-threshold setting.

$$Y(x) = \beta_0 + \beta_1 * \text{meanheight} + \beta_2 * \text{meanheight}^2 + \beta_3 * \text{stddev} + \beta_4 * \text{lidaryear}_1 + \dots + \beta_{12} * \text{lidaryear}_9 + \beta_{13} * \text{treespecies}_1 + \dots + \beta_{18} * \text{treespecies}_6 + e(x) \quad (1)$$

206 sample plots included no sample trees and the timber volume density $Y(x)$ was thus set to zero. These *zero-plots* were removed from the modeling dataset since they acted as leverage points in cases where the LiDAR height metrics were recorded long before the terrestrial survey. Together with the missing tree species information (section 2.3.2), the modeling dataset was limited to 5206 observations.

3 Results

3.1 Classification Accuracies

Effect of Support Size and Threshold

Before calibration, the lowest user's accuracies (*UA*) for most tree species were realized using high thresholds of 80% and 100% for deciding the main tree species on the plot level (figure 4a). A plausible reason for this is that raising the threshold to higher values (e.g. 80%, 100%) distinctively increases the probability of the reference class (based on the sample trees of the sample location) to be assigned as class 'Mixed', while the much coarser spatial resolution of the tree species map causes the *predicted* class to remain classified as one of the five tree species. However, as the support size is increased, so does the number of tree species raster cells to be evaluated at the sample location, thereby increasing the probability that the predicted class will be 'Mixed'. For this reason, most tree species exhibit an increase in user's accuracy under higher thresholds with higher support sizes. This scale-threshold dependency of the user's accuracy particularly affects tree species that most commonly occur in mixed forest stands in Rhineland-Palatinate (*Scots pine*, *oak* and *beech*), whereas the user's accuracies for tree species that are mostly prominent in pure forest stands (*spruce*, *Douglas fir*) logically turned out to be much more robust to changes in the thresholds and support sizes.

Among the uncalibrated tree species predictions, *beech* and *spruce* produced the best predictions achieving UAs of up to 70% and 80%. Although the predictions for *Douglas fir* and *Scots pine* generally performed less well than *beech* and *spruce*, similar UAs can be produced by adjusting the threshold and support choices. UAs for *oak* never performed

better than 50%. A detailed table of the user's and overall accuracies is provided in Online Resource 3.

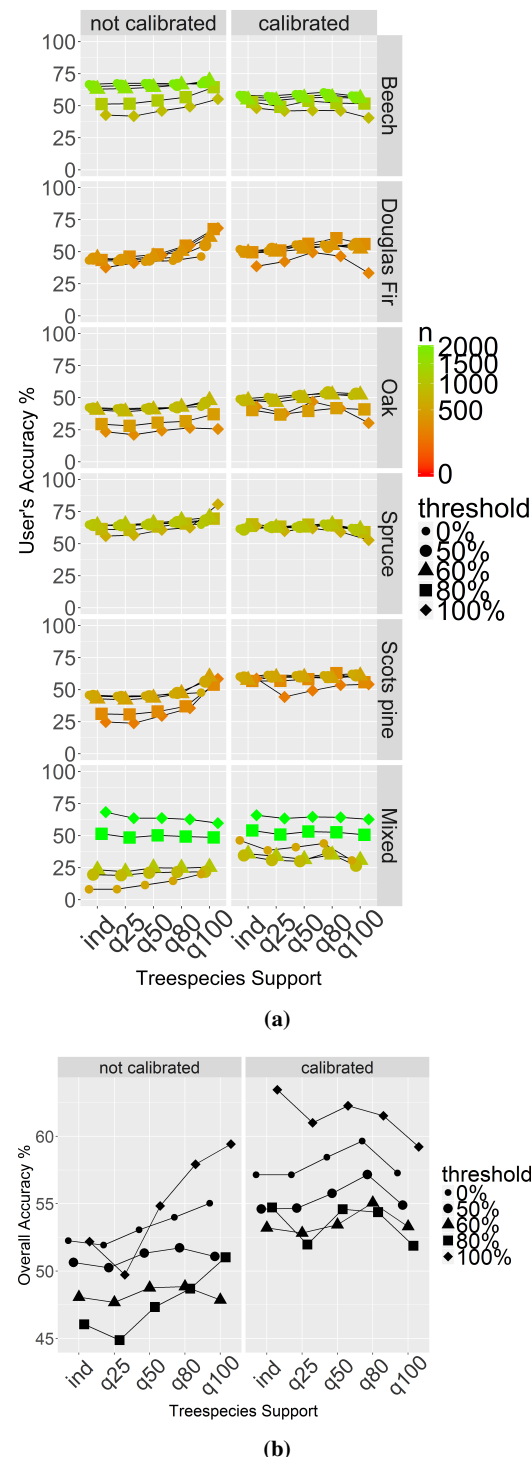


Fig. 4: Classification accuracy for the main tree species of a sample location *before* and *after* calibration: a) user's accuracies. b) overall accuracies. n: number of validation data per class

1 Effect of Calibration

2
 3 Calibration substantially diminished the effect of the scale-
 4 threshold dependency for the five tree species and also in-
 5 creased the UAs for *Scots pine* and *oak*. Whereas the UA
 6 level of *spruce* remained unchanged, the UAs for *beech*
 7 were found to be slightly lower after calibration. The overall
 8 accuracy under each support choice was always consider-
 9 ably increased by calibrating the tree species prediction (fig-
 10 ure 4b). With respect to the calculated random forest mod-
 11 els, the initial tree species prediction (*treespecies*) and the
 12 information about the growing region (*wgb*) turned out to
 13 be the most valuable information, followed by the estimated
 14 proportion of coniferous trees (*prop.conif*) and the mean
 15 canopy height (*meanheight*).
 16
 17

20 3.2 Regression Model Accuracies

22 Effect of Support Size and Threshold

24 Figure 5 shows the accuracies of the regression model (equa-
 25 tion 1) achieved under all possible combinations of support
 26 sizes for the auxiliary data. The stepwise selection procedure
 27 always included all considered single and interaction terms.
 28 In terms of adjusted R^2 and $RMSE_{cv}$, the analysis revealed
 29 that the choice of the CHM support size controls the over-
 30 all level of the model's accuracy. The information about the
 31 main plot tree species can then be used to further improve
 32 the model fit under suitable *treespecies* support and thresh-
 33 old settings. When using the uncalibrated *treespecies* vari-
 34 able, an increase of the *treespecies* support size causes an in-
 35 crease in the model performance if low thresholds are used,
 36 whereas high thresholds (80%, 100%) cause a decrease in
 37 the model performance. This threshold-dependency could
 38 be removed by calibrating the *treespecies* variable. The
 39 highest adjusted R^2 and the lowest $RMSE_{cv}$ were realized
 40 using the *q50* support for the CHM variables in combina-
 41 tion with the *q100* support and a threshold of 100% for
 42 the calibrated *treespecies* variable (adjusted $R^2=0.49$ and
 43 $RMSE_{cv}=132 \text{ m}^3/\text{ha}$). However, various support and thresh-
 44 old combinations for the CHM and *treespecies* variables can
 45 be used to yield almost identical $RMSE_{cv}$ and adjusted R^2
 46 values. A detailed table of the model accuracies is given in
 47 Online Resource 4.
 48
 49

52 Effect of Misclassifications

54 We can assess magnitude of the misclassification effect by
 55 comparing the adjusted R^2 's of models that use the predicted
 56 tree species (calibrated and uncalibrated) as an explanatory
 57 variable to models that use the error-free tree species vari-
 58 ables acquired from the terrestrial survey. Note that only the
 59 variables acquired from the terrestrial survey. Note that only the
 60 variables acquired from the terrestrial survey. Note that only the
 61 variables acquired from the terrestrial survey. Note that only the
 62 variables acquired from the terrestrial survey. Note that only the
 63 variables acquired from the terrestrial survey. Note that only the
 64 variables acquired from the terrestrial survey. Note that only the
 65 variables acquired from the terrestrial survey.
 66

model with the predicted tree species variables can be applied to additional sample locations where no terrestrial survey has been carried out. Figure 6 provides a comparison of the adjusted R^2 achieved under the use of the error-free tree species predictor variable against the adjusted R^2 realized under the use of the tree species variable containing misclassifications. This analysis was carried out for all models that were analysed in section 3.2, i.e. for all possible support and threshold combinations for the CHM and *treespecies* predictor variables.

As expected, the highest adjusted R^2 for every evaluated model was always achieved using the error-free tree species variable, whereas the misclassifications in the tree species variable led to a systematic decrease of the model accuracy. This is in agreement with the potential effects of erroneous explanatory variables discussed in Carroll et al (2006) and Gustafson (2003), i.e. an increase of variability (noise) in the data that can increase the amount of unexplainable variance and thereby reduce the model accuracy.

The calibration of the initially predicted main plot tree species using the random forest classification algorithm (section 2.3.2) turned out to not only improve the classification accuracies (section 3.1), but also to considerably decrease the effect of the misclassifications on the regression model predictions and accuracy. Figure 6 (right) shows that the adjusted R^2 under the actual and the calibrated predicted tree species variable are in general much closer to, and in many cases even on the identity line. Whereas the misclassifications in the uncalibrated *treespecies* variable led to a residual inflation of 1% - 5%, it was only between 0% and 1% after calibration. Further analysis revealed that when using the calibrated *treespecies* variables, the regression coefficients were almost identical to the ones received using the actual main plot tree species.

3.3 Final Regression Model

In order to address research questions 1 and 2 (i.e. the gain in model accuracy by tree species information and effect of heterogeneity in the LiDAR data), we investigated the model properties in more detail. For this purpose, we decided to use the support settings of *q50* for both auxiliary data with a threshold of 100% for the tree species variable as the regression model of choice. The reason for this choice was that *a*) the model provided almost the highest adjusted R^2 among all validated models while reducing the data handling complexity for upcoming applications (i.e. identical support sizes for all remote sensing data) and *b*) the calibration neutralized the effects of misclassifications on the model predictions. The interaction term between *meanheight*² and *treespecies* (i.e. considering separate curvatures for each tree species) turned out not to have any influence on the model accuracy

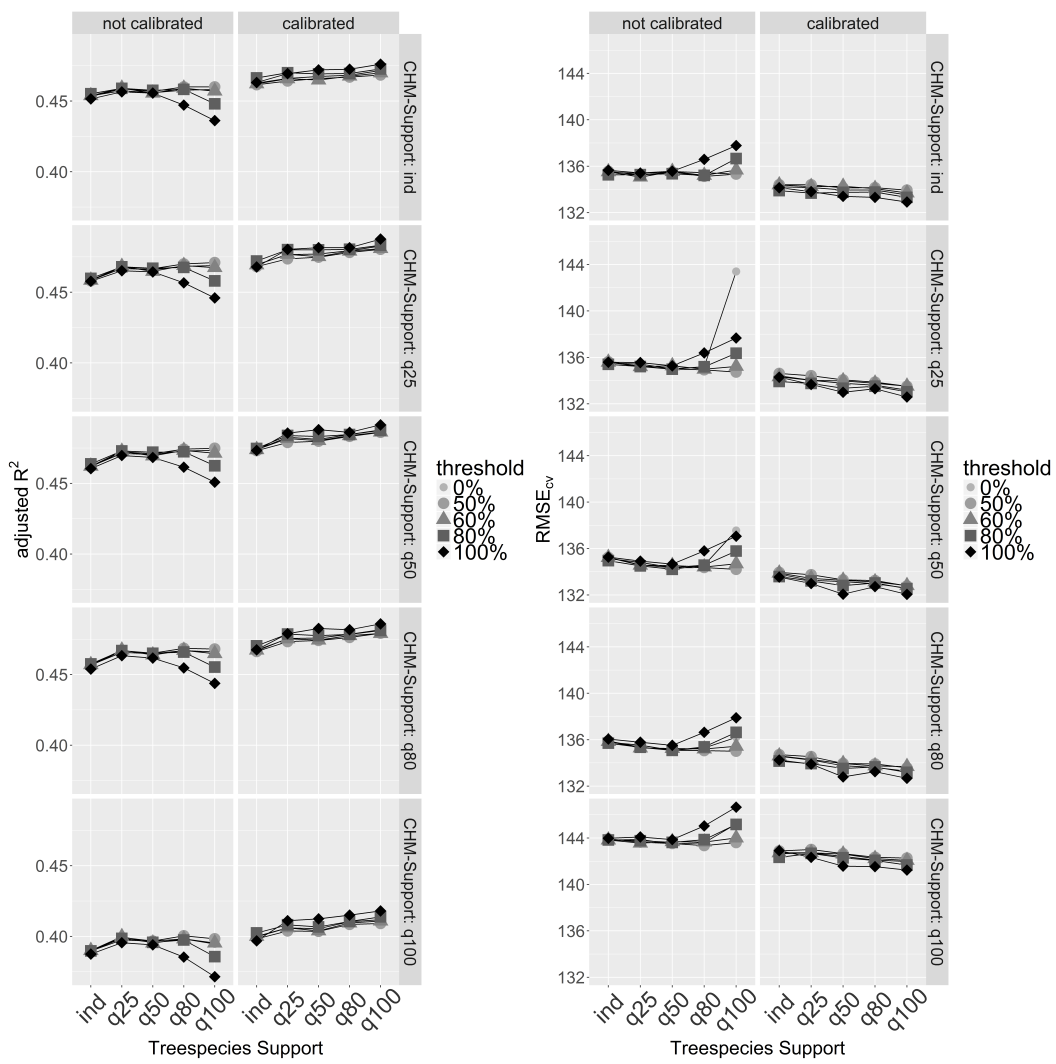


Fig. 5: 10-fold RMSE_{cv} and adjusted R^2 realized under various support choices for the CHM and *treespecies* explanatory variables

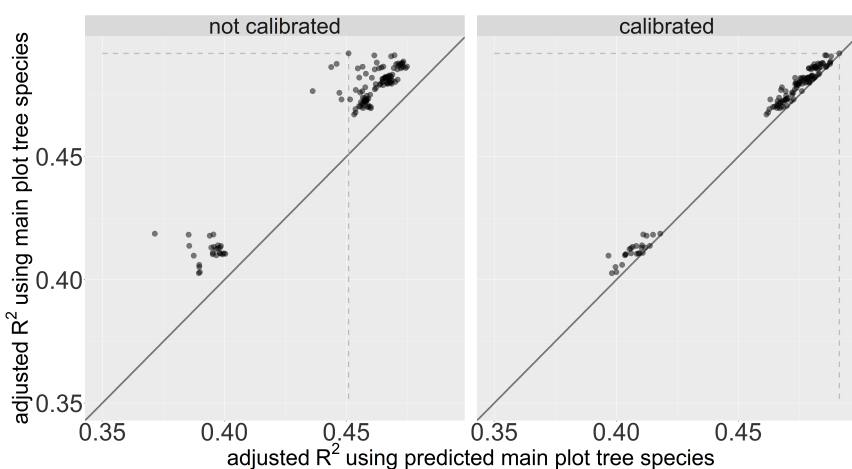


Fig. 6: Effect on the adjusted R^2 when substituting the actual main tree species with the predicted main tree species of a sample plot. The differentiation into two distinct point clouds results from the poor model performance under support size $q100$ for the CHM variables (i.e. the lower point cloud). The dotted line tracks the model with the highest adjusted R^2 under the use of the error-free *treespecies* variable

and was thus dropped, resulting in an adjusted R^2 of 0.49 and RMSE_{cv} of $132.12 \text{ m}^2/\text{ha}$.

Interpretation of Final Regression Model

Figure 7 provides a visualisation of the tree species prediction functions separated by the LiDAR acquisition years. Sample plots classified as *oak* and *Scots pine* revealed to have an almost identical relationship (nearly identical slopes) for the mean canopy height - timber volume relationship. They only differ by a marginally higher intercept for *Scots pine* plots, meaning that given the same mean canopy height a sample plot dominated by *Scots pine* yields a marginally higher timber volume on the plot level than a plot dominated by *oak*. *Beech*-dominated sample plots tend to achieve a higher timber volume than *oak* and *Scots pine* for canopy heights below 20 meters, but realize the lowest timber volumes for canopy heights above 20 metres. Sample plots dominated by any of the remaining coniferous tree species (*Douglas fir*, *spruce*) revealed to have higher slopes than broadleaf classified plots. This indicates that given the same mean canopy height, sample plots dominated by *Douglas fir* and *spruce* yield higher timber volume values than broadleaf- or *Scots pine* dominated sample plots, and this difference becomes more pronounced with increasing mean canopy heights. Within the group of coniferous-dominated sample plots, *spruce* turned out to have the highest slope, thereby yielding the highest timber volume values for mean canopy heights above 15 meters. An undesired characteristic of the model is that the predicted timber volume can in some cases (< 1%) take negative values for low canopy heights (e.g. for *spruce*-dominated plots with *meanheight* below 5 meters and *stddev* of 4 meters). However, we chose not to use a log-transformation of the response variable. Doing so would have prevented the subsequent calculation of the g-weight variance of the model assisted estimators (Mandalaz, 2013a; Mandallaz et al., 2013), which is only possible for response variables on the original scale.

Effect of Time-Lags and Heterogeneity in LiDAR Data

Incorporating the LiDAR acquisition year as a categorical variable (*lidaryear*) in the regression model substantially accounted for the variability in the data introduced by *a*) the time-lags between LiDAR acquisition and terrestrial survey, and *b*) variation in LiDAR data quality which are due to sensor- and post processing techniques (table 2). Whereas the adjusted R^2 for the regression model without considering the LiDAR acquisition year as additional predictor variable was 0.35 (0.41 including the tree species variable), the stratification by the LiDAR acquisition year led to adjusted R^2 of 0.44 (0.48), thereby increasing the proportion of explained variance by up to 9%.

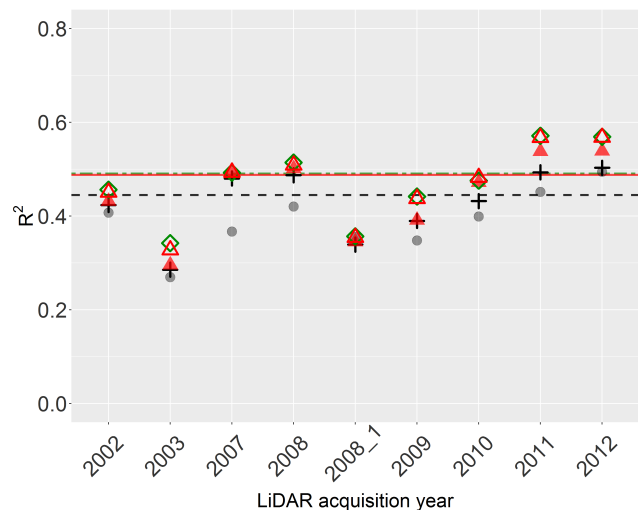


Fig. 8: R^2 of the final regression model achieved *within* the LiDAR acquisition year strata. Grey points: R^2 of submodel 1 (no stratification according to LiDAR acquisition year or tree species). Crosses: R^2 of submodel 2 (*without* tree species stratification). Filled triangles: R^2 of final model using the *uncalibrated* tree species variable. Empty triangles: R^2 of final model using the *calibrated* tree species variable. Diamonds: R^2 achieved using the *error-free* tree species variable (derived from sample trees). Dotted line: Overall adjusted R^2 of submodel 2. Solid line: Overall adjusted R^2 of final model using the *calibrated* tree species variable. Two-dashed line: Overall adjusted R^2 of final model using the *error-free* tree species variable

Table 1: R^2 , RMSE and Residual Square Sum (SSE) of final regression model within LiDAR acquisition year strata (*lidaryear*). *n*: number of validation data

LiDAR acquisition year	R^2	rmse	SSE	<i>n</i>
2012	0.57	135.20	7073596	387
2011	0.57	136.41	15779849	848
2010	0.48	119.57	16199324	1133
2009	0.44	122.87	8077013	535
2008	0.51	121.15	9936203	677
2008_1	0.35	158.76	9678912	384
2007	0.49	127.71	6736041	413
2003	0.33	142.24	10521254	520
2002	0.45	135.08	5638379	309

We further analysed the model residuals within each LiDAR acquisition year (within-group variation) for the final model and nested submodels. It turned out that the R^2 vary distinctly between the LiDAR acquisition year strata (figure 8). More precisely, the within-group R^2 can be higher and lower than the overall R^2 of the respective model. Figure 8 shows that a stratification according to the LiDAR acquisition years (submodel 2) can already increase the R^2 in most acquisition year strata, compared to the basic model using only the LiDAR height metrics as predictor variables (submodel 1). In some LiDAR acquisition year strata (i.e. 2007,

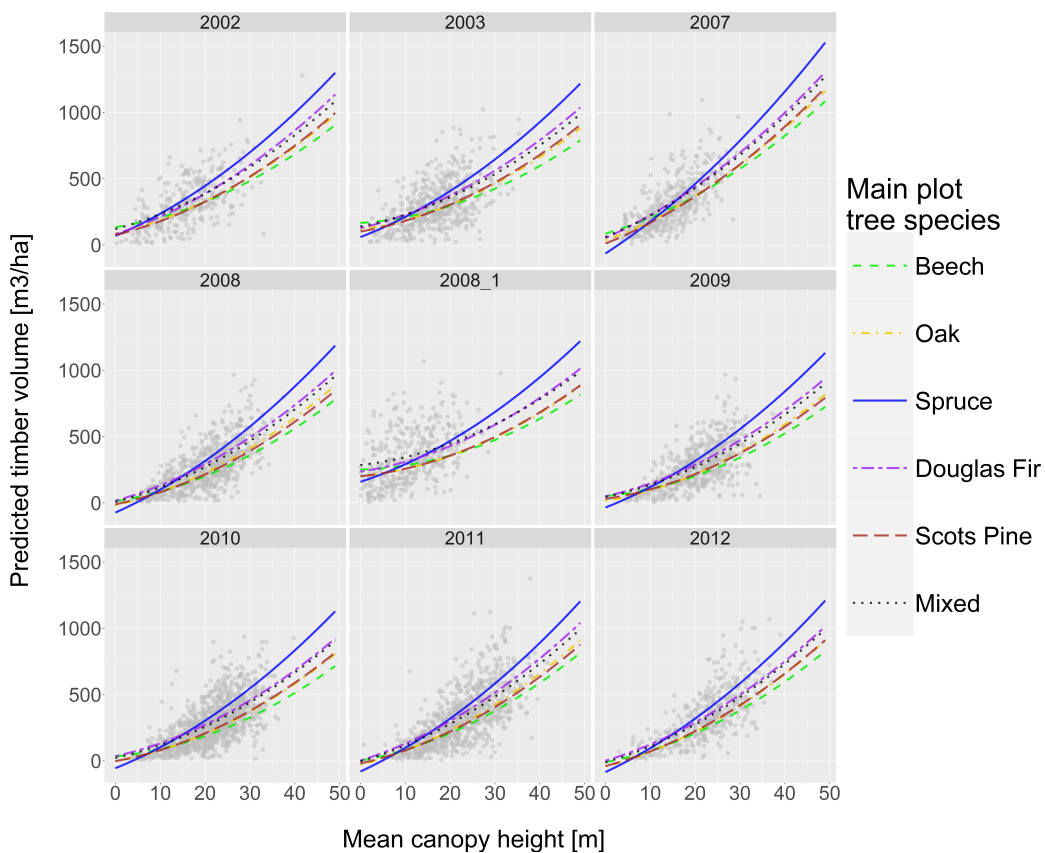


Fig. 7: Visualization of the timber volume prediction function (*final regression model*) on sample plot level for each main plot tree species and LiDAR acquisition year. For visualization purposes, the predictor variable *stddev* was set to its average value within the respective *treespecies* and *lidaryear* group

2008), this increase in R^2 even reached 8% - 13%. The accuracies for the final model are also given in table 1.

Added Value of Tree Species Map Information

Using the predicted main tree species of a sample plot as an additional categorical variable yielded a further increase of the model accuracy of 6% in the R^2 (table 2). This improvement was particularly pronounced in LiDAR acquisition years that are close or identical to the year of the terrestrial inventory (R^2 of 0.57 in 2011 and 2012, figure 8). The analysis illustrated once more that misclassifications in the tree species variable generally reduce model accuracy compared to using error-free tree species information. The residual inflations caused by the misclassifications in the uncalibrated *treespecies* variable within the *lidaryear* strata were up to 5%. However, the calibration was able to substantially decrease or even remove the effects of misclassifications on the model accuracy in all LiDAR acquisition year strata.

4 Discussion

4.1 Stratification according to Tree Species and LiDAR Acquisitions

Incorporating the main tree species of a sample location in the timber volume regression model significantly increased the model accuracy and revealed strong evidence for the existence of a tree species specific behaviour concerning timber volume on the plot level. This result seems reasonable regarding the species specific taper functions on single-tree level applied in the BWI3 (Kublin, 2003; Kublin et al, 2013). Further evidence and specification of the tree species effects on sample plot level - up to modeling individual tree species - would be desirable. However, this was not possible in our study because the stratification according to the LiDAR acquisition years severely limited the flexibility of species-specific prediction functions and model interpretability. In particular, using the LiDAR acquisition years as categorical variables led to highly unbalanced datasets when stratifying according to the main plot tree species, and prevented the use of further stratification variables such as bioclimatic growing regions due to confounding effects and consequent

Table 2: Accuracy metrics for submodels of final OLS regression model

model terms	model	parameters	R^2_{adj}	$RMSE_{cv}$
meanheight + stddev + meanheight ² + treespecies + lidaryear + meanheight:treespecies + meanheight:lidaryear + meanheight:stddev + stddev:lidaryear	final model	39	0.49	132.12
meanheight + stddev + meanheight ² + meanheight:stddev	submodel 1	5	0.35	148.03
meanheight + stddev + meanheight ² + lidaryear + meanheight:lidaryear + meanheight:stddev + stddev:lidaryear	submodel 2	29	0.44	137.52
meanheight + stddev + meanheight ² + treespecies + meanheight:treespecies + meanheight:stddev	submodel 3	15	0.41	137.52

singularities in the design matrices. A stratification to the LiDAR acquisition years however proved to be a means in accounting for the artificially introduced noise in the data caused by quality variations and the large time-lags between the remote sensing and terrestrial data. Incorporating the calibrated tree species information further improved the model accuracy by 6% in adjusted R^2 . Compared to the simple model only containing LiDAR height metrics, including the LiDAR quality and calibrated tree species information increased the adjusted R^2 by 14%. A differentiated evaluation revealed that the R^2 within LiDAR acquisitions year strata identical with the year of the terrestrial survey were much higher than those of previous acquisition years, showing differences of up to 22% between the R^2 's (0.35 compared to 0.57, table 2). The gain in the R^2 and the prediction performance when including the tree species information was also largest in combination with LiDAR information acquired in the year of the terrestrial inventory. These insights were also particularly interesting with respect to the further use of the regression model for small area estimations. Small area estimators generally gain modeling strength by defining the prediction model *globally* (i.e. using all data in the inventory area), and then applying the so-derived prediction model to a subset of observations located within the area of interest (Mandallaz et al., 2016). Consequently, the proposed stratification technique in the prediction model could be expected to yield a gain in model accuracy and a reduction of the small area estimation errors if the small area domain mostly includes data from strata that have high within-strata model accuracies. This hypothesis is subject to ongoing analysis.

4.2 Calibration of Tree Species Map Information

The accuracy assessment of the initially derived main plot species from the classification map revealed the presence of misclassifications that led to a decrease in model accuracy.

One reason for the misclassifications were that the classification algorithm of Stoffels et al (2015) was exclusively trained in pure stands with the objective to predict the *dominant tree species* of a forest stand. Thus, our requirements on the classification map differed considerably from the ones imposed by Stoffels et al (2015) and have to be considered as far more difficult to meet. Firstly, the reference data used in the accuracy assessment also included understory trees that were recorded in the BWI3 sample. Secondly, determining an exact spatial validation unit for a sample location (support) is not possible due to the properties of angle count sampling (section 2.4). Thirdly, distinct discrepancies in the spatial scale between the reference data and the classification map severely hamper exact predictions of the main plot tree species especially in mixed forest stands. The latter issue caused a pronounced dependency of the user's accuracy on the support and threshold choice, particularly for tree species that most commonly occur in mixed forest structures, i.e. *Scots pine* (91%), *oak* (90%) and *beech* (85%) (von Thünen-Institut, 2014). With respect to this set-up, the application of our calibration method proved to be of high value. It led to an increase in the classification accuracies, particularly for those tree species that performed worse in the uncalibrated setup, and thereby successfully minimized and even removed the deleterious effect of misclassifications on model accuracy and regression coefficients. We consider this *a posteriori calibration* a valuable method for future studies where an external tree species map (i.e. the map was not created for the specific study objective) is used in prediction models. Whereas the extensive analysis in our study deepened the understanding of the afore mentioned scale-effects, an alternative method for future applications could be to use map-derived percentages of each tree species as predictor variables in the random forest algorithm in order to directly predict the terrestrially observed main plot tree species.

1 2 3 4 5 6 7 8 9 10 11 12 13 14 15 16 17 18 19 20 21 22 23 24 25 26 27 28 29 30 31 32 33 34 35 36 37 38 39 40 41 42 43 44 45 46 47 48 49 50 51 52 53 54 55 56 57 58 59 60 61 62 63 64 65 4.3 Choice of Support under Angle Count Sampling

The validation of different support sizes underlined that the support choice can impact prediction accuracy. In the present study, differences in the model accuracies turned out to be small for most support choices. An exception was the choice of the q_{100} support for the CHM derived variables (76 meter side length), where the model accuracy was considerably worse than what was achieved under optimal settings. With the exception of the latter, the accuracy differences according to adjusted R^2 and RMSE_{cv} were very similar to those found by Deo et al (2016) when evaluating the model performance of optimal support sizes for a range of various basal area factors. An analysis to find the best support settings therefore seems to be advisable prior to further applications of model-assisted or model-dependent inventory methods so as not to lose model accuracy by unsuitable support choices. The concept of the demonstrated analysis method for identifying suitable supports can be transferred to any kind of auxiliary information, predictor variable and prediction model.

Contrary to our hypothesis, the use of plot-individual supports did not yield the best prediction performances. A plausible reason for this is that determining an exact plot radius under angle count sampling is technically infeasible, and thus, angle count sampling does not seem to be adequate when linking inventory information with remote sensing data. It has already been indicated that using predictor variables derived from auxiliary data of much higher spatial resolution than those used in this study (e.g. based on individual tree detections) will require supports that correspond not only to the actual spatial extent, but also to the exact position of the sample locations (Lamprecht et al, 2017). However, the extensive analysis carried out in our study indicated that the optimal support size depends on the spatial resolution of the remote sensing data as well as the context in which the derived information is used in the prediction model. In the case of transforming the tree species information map into a suitable categorical predictor variable, the use of a large support size of 76 meter side length turned out to yield the best model accuracy. However, only few sample locations in the study area were actually characterized by limiting circles of that particular size.

5 Conclusion

The objective of this study was to identify a suitable ordinary least square regression model that can be applied over the entire forest area of Rhineland-Palatinate using model-assisted estimators. The large amount of data that was gathered in the frame of this study allowed for extensive modeling possibilities, but had the side effect of contributing

to high heterogeneity in the response and explanatory variables. Whereas the variability of the response variable (timber volume on plot level) is due to the very heterogeneous forest structures and bioclimatic growing regions in RLP, a considerable amount of heterogeneity in the explanatory variables was introduced by quality restrictions in the remote sensing data. This was particularly true for the LiDAR derived canopy height information that was gathered in a time span of ten years around the date of the terrestrial inventory and revealed pronounced quality variations. With an adjusted R^2 of 0.49 and a RMSE_{cv} of $132 \text{ m}^3/\text{ha}$, the model accuracy was still very close to those found in similar studies (Maack et al, 2016). Our analyses strongly indicate that the acquisition of the auxiliary information close to the date of the terrestrial survey is a key factor in order to increase the model accuracy. We also expect the tree species information in the timber volume model to become even more relevant if the temporal synchronicity and the quality of the canopy height information is improved. An up-to-date canopy height model would also circumvent a stratification according to different LiDAR acquisition characteristics, lead to a more balanced dataset when stratifying for the main plot tree species and allow for incorporating information that can further explain the variation within each tree species group. With respect to the latter, information about the bioclimatic growing conditions, soil properties and the stand density on plot level are expected to further improve the model's predictive performance. Promising steps with respect to more up-to-date auxiliary information have already been made, as the topographic survey institution of RLP is currently processing a canopy height model from aerial imagery acquisitions for 2011 and 2012 covering the entire federal state. These aerial photography acquisitions will in the future be conducted in a two-year period, allowing to derive up-to-date canopy height information in the framework of future forest inventories. As the availability of countrywide imagery-based surface models has been increasing (Ginzler and Hobi, 2015), investigating the performance between areal and LiDAR derived canopy height models and their consequent predictive power in the frame of timber volume estimations (Ullah et al, 2017) are tasks for subsequent analysis. Additionally, availability of satellite data for tree species classification map production with respect to up-to-dateness and coverage has recently been increasing in the frame of the Sentinel-2 mission (ESA, 2017).

Acknowledgements We want to express our gratitude to Prof. H. Heinemann (Chair of Land Use Engineering, ETH Zurich) for supporting this study. We want to explicitly thank Dr. Johannes Stoffels from the Environmental Sensing and Geoinformatics Group of Trier University for providing the tree species classification map as well as for constructive discussions when it came to interpreting the results. Special gratitude is owed to the State Forest Service of Rhineland-Palatinate, in particular Dr. Joachim Langshausen, Jürgen Dietz and Claus-Andreas Lessander, for collaboration and providing the forest inventory and geodata. We also want to thank Kai Husmann and Christoph Fischer from the Northwest German Forest Research Institution Göttingen for their advice in processing the terrestrial inventory data, and Alexander Massey and Michael Hill for proofreading.

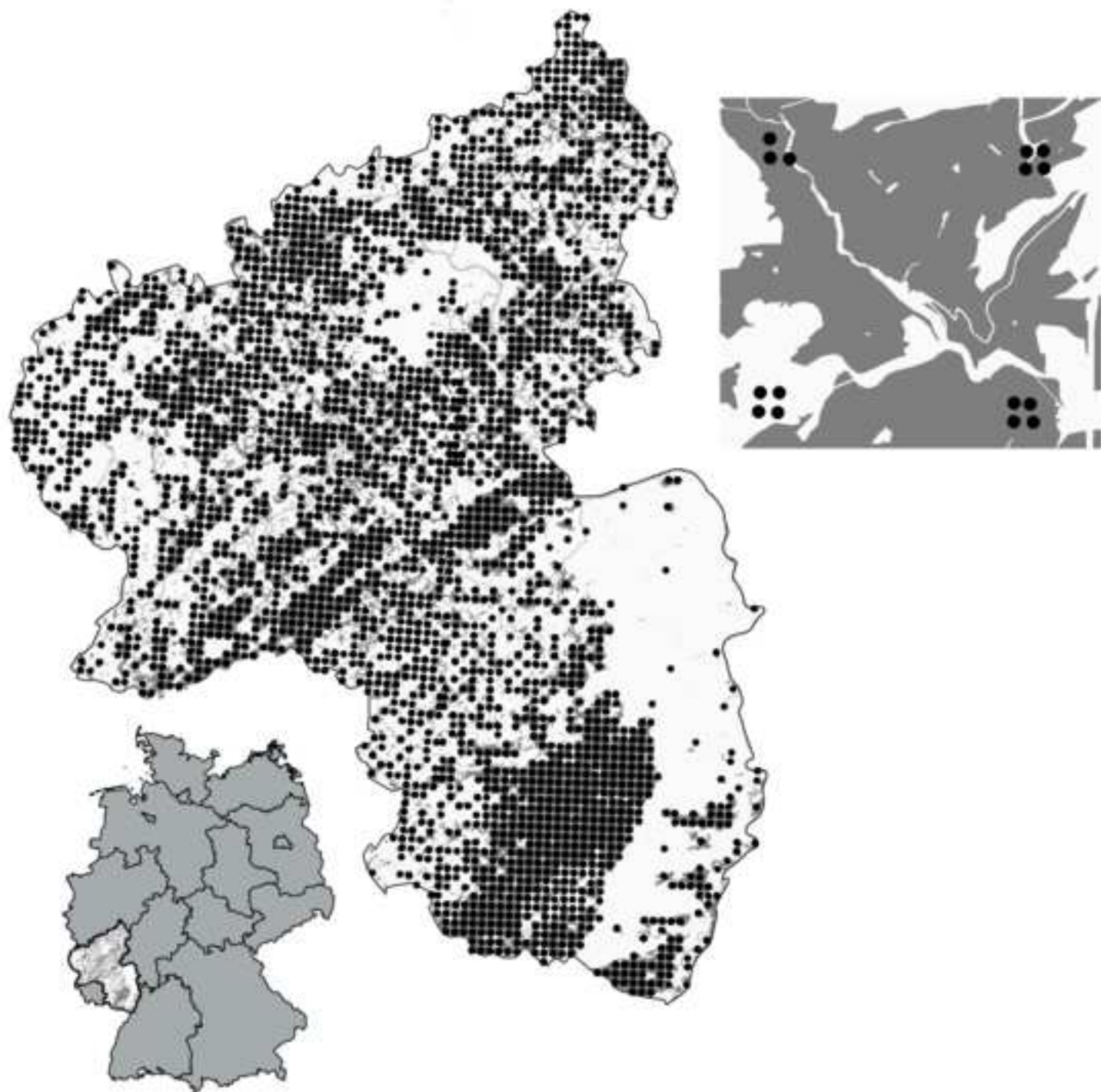
Conflict of Interest The authors declare that they have no conflict of interest.

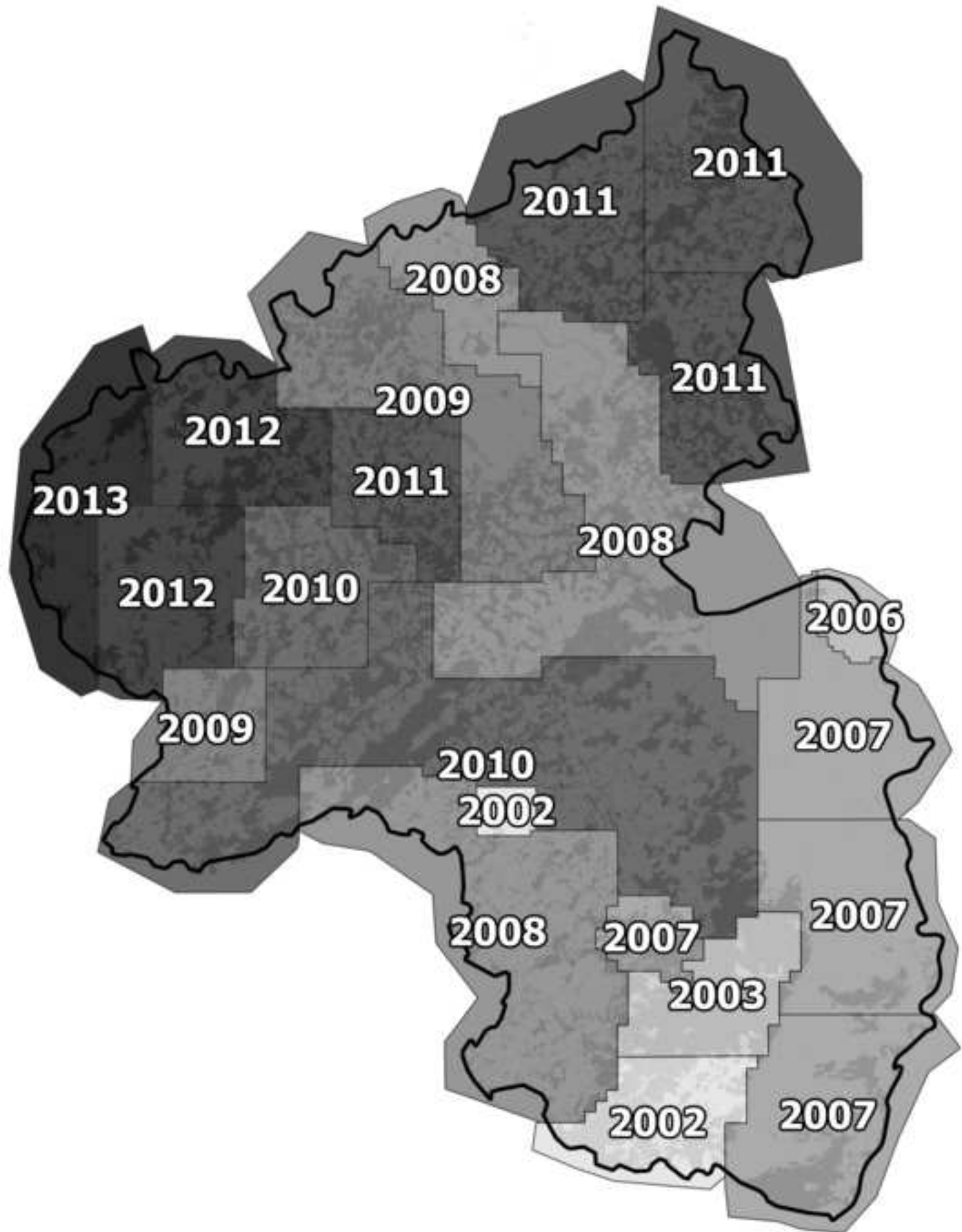
References

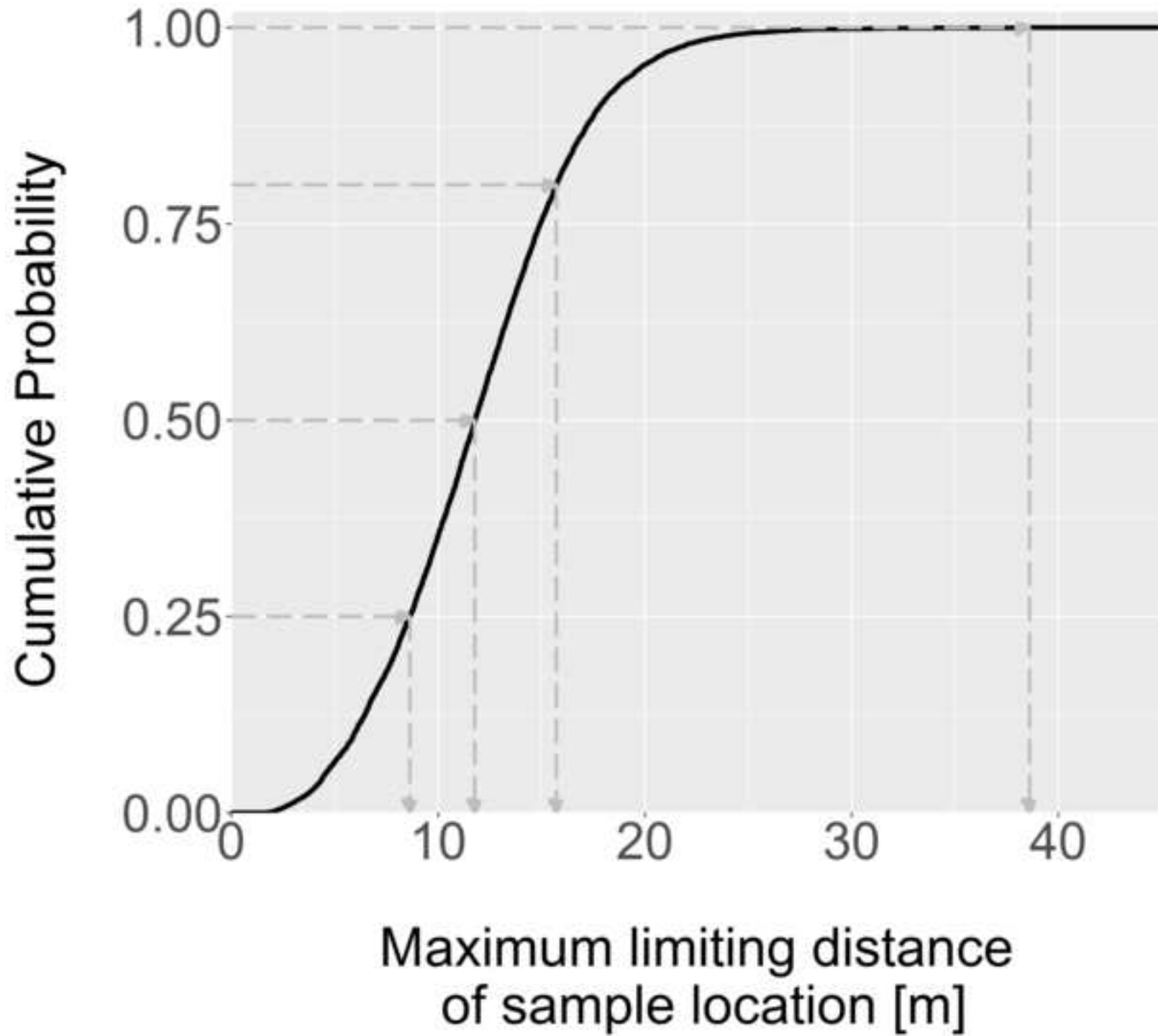
- Akaike H (2011) Akaike's Information Criterion, Springer Berlin Heidelberg, Berlin, Heidelberg, pp 25–25. DOI 10.1007/978-3-642-04898-2_110, URL http://dx.doi.org/10.1007/978-3-642-04898-2_110
- Beaudoin A, Bernier P, Guindon L, Villemaire P, Guo X, Stinson G, Bergeron T, Magnussen S, Hall R (2014) Mapping attributes of Canada's forests at moderate resolution through k nn and modis imagery. Canadian Journal of Forest Research 44(5):521–532, DOI 10.1139/cjfr-2013-0401, URL <https://doi.org/10.1139/cjfr-2013-0401>
- Bitterlich W (1984) The relascope idea. Relative measurements in forestry. Commonwealth Agricultural Bureaux
- Breidenbach J, Astrup R (2012) Small area estimation of forest attributes in the norwegian national forest inventory. European Journal of Forest Research 131(4):1255–1267, DOI 10.1007/s10342-012-0596-7
- Breiman L (2001) Random forests. Machine learning 45(1):5–32, DOI 10.1023/A:1010933404324
- Carroll RJ, Ruppert D, Stefanski LA, Crainiceanu CM (2006) Measurement error in nonlinear models: a modern perspective. CRC press, DOI 10.1201/9781420010138, URL <https://doi.org/10.1201/9781420010138>
- Congalton RG, Green K (2008) Assessing the accuracy of remotely sensed data: principles and practices. CRC press, DOI 10.1201/9781420055139, URL <https://doi.org/10.1201/9781420055139>
- Deo RK, Froese RE, Falkowski MJ, Hudak AT (2016) Optimizing variable radius plot size and lidar resolution to model standing volume in conifer forests. Canadian Journal of Remote Sensing 42(5):428–442, DOI 10.1080/07038992.2016.1220826, URL <http://dx.doi.org/10.1080/07038992.2016.1220826>, <http://dx.doi.org/10.1080/07038992.2016.1220826>
- Bundesministerium für Ernährung LuV (2011) Aufnahmeanweisung für die dritte Bundeswaldinventur BWI3 (2011 - 2012). URL <https://www.bundeswaldinventur.de/index.php?id=421>
- ESA (2017) Sentinel-2 earth observation mission. URL http://www.esa.int/Our_Activities/Observing_the_Earth/Copernicus/Sentinel-2, accessed: 2017-03-29
- Gauer J, Aldinger E (2005) Waldökologische Naturräume Deutschlands-Wuchsgebiete. Mitteilungen des Vereins für Forstliche Standortskunde und Forstpflanzenzüchtung 43:281–288
- Ginzler C, Hobi ML (2015) Countrywide stereo-image matching for updating digital surface models in the framework of the swiss national forest inventory. Remote Sensing 7(4):4343–4370, DOI 10.3390/rs70404343, URL <http://www.mdpi.com/2072-4292/7/4/4343>
- Gregoire TG, Valentine HT (2007) Sampling strategies for natural resources and the environment. CRC Press
- Gustafson P (2003) Measurement error and misclassification in statistics and epidemiology: impacts and Bayesian adjustments. CRC Press, DOI 10.1201/9780203502761, URL <https://doi.org/10.1201/9780203502761>
- Hill A, Breschan J, Mandallaz D (2014) Accuracy assessment of timber volume maps using forest inventory data and lidar canopy height models. Forests 5(9):2253–2275, DOI 10.3390/f5092253, URL <http://www.mdpi.com/1999-4907/5/9/2253>
- Hollaus M, Wagner W, Maier B, Schadauer K (2007) Airborne laser scanning of forest stem volume in a mountainous environment. Sensors 7(8):1559–1577, DOI 10.3390/s7081559, URL <http://www.mdpi.com/1424-8220/7/8/1559>
- Husmann K, Rumpf S, Nagel J (2017) Biomass functions and nutrient contents of European beech, oak, sycamore maple and ash and their meaning for the biomass supply chain. Journal of Cleaner Production DOI 10.1016/j.jclepro.2017.03.019, URL <https://doi.org/10.1016/j.jclepro.2017.03.019>
- Jakubowski MK, Guo Q, Kelly M (2013) Tradeoffs between lidar pulse density and forest measurement accuracy. Remote Sensing of Environment 130:245–253, DOI 10.1016/j.rse.2012.11.024, URL <https://doi.org/10.1016/j.rse.2012.11.024>
- Koch B (2010) Status and future of laser scanning, synthetic aperture radar and hyperspectral remote sensing data for forest biomass assessment. ISPRS Journal of Photogrammetry and Remote Sensing 65(6):581–590, DOI 10.1016/j.isprsjprs.2010.09.001, URL <https://doi.org/10.1016/j.isprsjprs.2010.09.001>
- Köhl M, Magnussen SS, Marchetti M (2006) Sampling methods, remote sensing and GIS multiresource forest inventory. Springer Science & Business Media

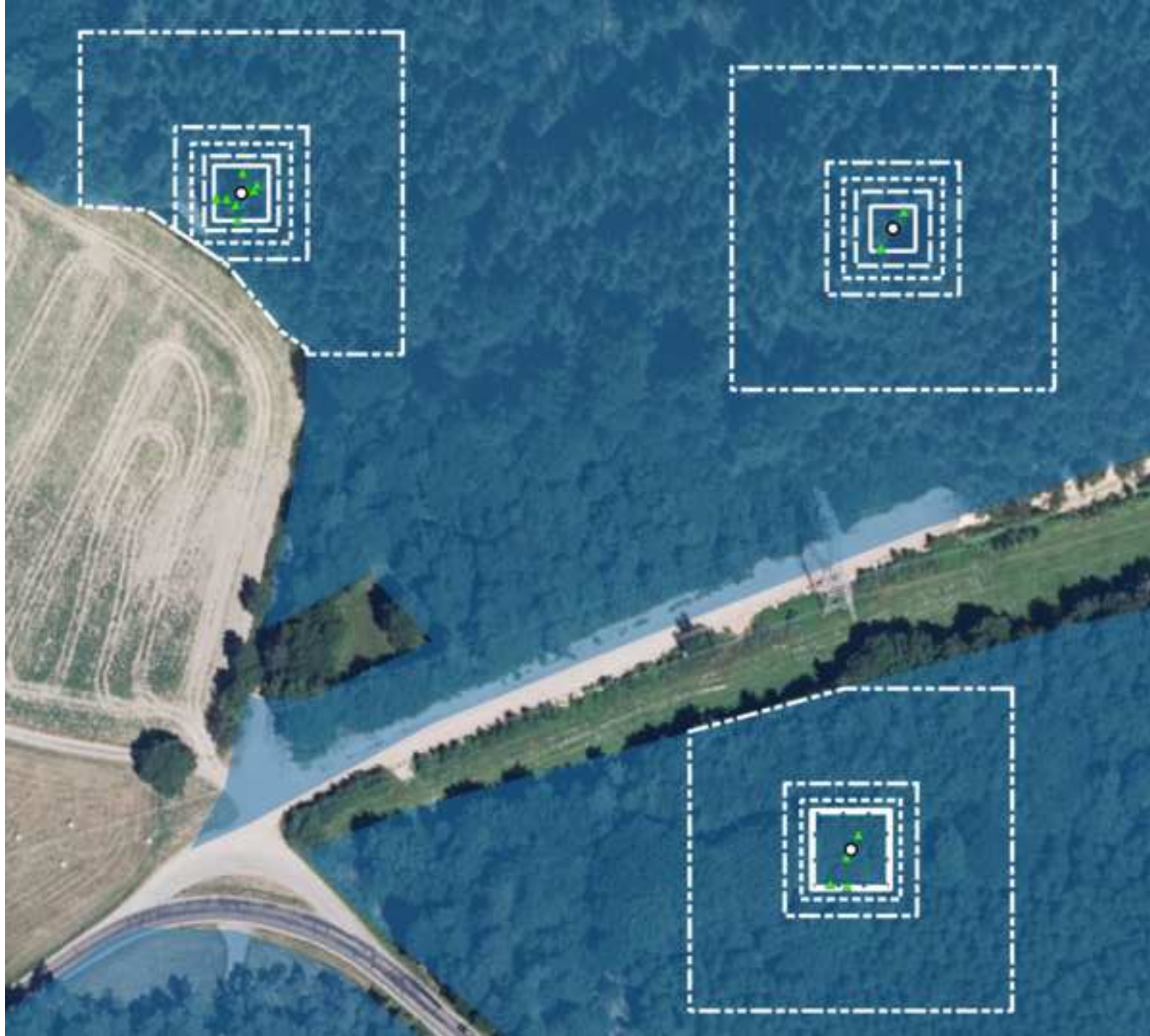
- 1 Kublin E (2003) Einheitliche beschreibung der
2 schaftform-methoden und programme-bdatpro.
3 Forstwissenschaftliches Centralblatt 122(3):183–200
4
- 5 Kublin E, Breidenbach J, Kändler G (2013) A flexi-
6 ble stem taper and volume prediction method based
7 on mixed-effects b-spline regression. European journal
8 of forest research 132(5-6):983–997, DOI 10.1007/
9 s10342-013-0715-0
- 10 Lamprecht S, Hill A, Stoffels J, Udelhoven T (2017) A ma-
11 chine learning method for co-registration and individual
12 tree matching of forest inventory and airborne laser scan-
13 ning data. Remote Sensing 9(5), DOI 10.3390/rs9050505,
14 URL <http://www.mdpi.com/2072-4292/9/5/505>
- 15 Latifi H, Nothdurft A, Koch B (2010) Non-parametric pre-
16 diction and mapping of standing timber volume and
17 biomass in a temperate forest: application of multiple
18 optical/lidar-derived predictors. Forestry 83(4):395–407,
19 DOI 10.1093/forestry/cpq022, URL <https://doi.org/10.1093/forestry/cpq022>
- 20 Latifi H, Nothdurft A, Straub C, Koch B (2012) Mod-
21 elling stratified forest attributes using optical/lidar fea-
22 tures in a central european landscape. International
23 Journal of Digital Earth 5(2):106–132, DOI 10.1080/
24 17538947.2011.583992, URL <http://dx.doi.org/10.1080/17538947.2011.583992>
- 25 Liaw A, Wiener M (2002) Classification and regression by
26 randomforest. R News 2(3):18–22, URL <http://CRAN.R-project.org/doc/Rnews/>
- 27 von Lüpke N, Saborowski J (2014) Combining double
28 sampling for stratification and cluster sampling to a
29 three-level sampling design for continuous forest inven-
30 tories. European journal of forest research 133(1):89–
31 100, DOI 10.1007/s10342-013-0743-9, URL <http://dx.doi.org/10.1007/s10342-013-0743-9>
- 32 Maack J, Lingenfelder M, Weinacker H, Koch B (2016) Modelling the standing timber volume of baden-
33 württemberg—a large-scale approach using a fusion of
34 landsat, airborne lidar and national forest inventory data.
35 International Journal of Applied Earth Observation and
36 Geoinformation 49:107–116, DOI 10.1016/j.jag.2016.02.
37 004, URL <https://doi.org/10.1016/j.jag.2016.02.004>
- 38 Magnussen S, Næsset E, Gobakken T (2010) Reliability of
39 lidar derived predictors of forest inventory attributes: A
40 case study with norway spruce. Remote Sensing of En-
41 vironment 114(4):700–712, DOI 10.1016/j.rse.2009.11.
42 007, URL <https://doi.org/10.1016/j.rse.2009.11.007>
- 43 Magnussen S, Mandallaz D, Breidenbach J, Lanz A, Gin-
44 zler C (2014) National forest inventories in the ser-
45 vice of small area estimation of stem volume. Canadian
46 Journal of Forest Research 44(9):1079–1090, DOI
47 10.1139/cjfr-2013-0448, URL <https://doi.org/10.1139/cjfr-2013-0448>
- 48 Mandallaz D (2008) Sampling techniques for forest inven-
49 tories. CRC Press, DOI 10.1201/9781584889779, URL
50 <https://doi.org/10.1201/9781584889779>
- 51 Mandallaz D (2013a) Design-based properties of some
52 small-area estimators in forest inventory with two-
53 phase sampling. Canadian Journal of Forest Re-
54 search 43(5):441–449, DOI 10.1139/cjfr-2012-0381,
55 URL <https://doi.org/10.1139/cjfr-2012-0381>
- 56 Mandallaz D (2013b) A three-phase sampling exten-
57 sion of the generalized regression estimator with par-
58 tially exhaustive information. Canadian Journal of Forest
59 Research 44(4):383–388, DOI 10.1139/cjfr-2013-0449,
60 URL <https://doi.org/10.1139/cjfr-2013-0449>
- 61 Mandallaz D, Breschan J, Hill A (2013) New regression es-
62 timators in forest inventories with two-phase sampling and
63 partially exhaustive information: a design-based monte
64 carlo approach with applications to small-area estimation.
65 Canadian Journal of Forest Research 43(11):1023–1031,
DOI 10.1139/cjfr-2013-0181, URL <https://doi.org/10.1139/cjfr-2013-0181>
- 66 Mandallaz D, Hill A, Massey A (2016) Design-based prop-
67 erties of some small-area estimators in forest inventory
68 with two-phase sampling - revised version. Tech. rep.,
69 Department of Environmental Systems Science, ETH
70 Zurich, DOI 10.3929/ethz-a-010579388, URL <https://doi.org/10.3929/ethz-a-010579388>
- 71 Massey A, Mandallaz D (2015) Design-based regres-
72 sion estimation of net change for forest inventories.
73 Canadian Journal of Forest Research 45(12):1775–
74 1784, DOI 10.1139/cjfr-2015-0266, URL <https://doi.org/10.1139/cjfr-2015-0266>, <https://doi.org/10.1139/cjfr-2015-0266>
- 75 Massey A, Mandallaz D, Lanz A (2014) Integrating re-
76 mote sensing and past inventory data under the new an-
77 nual design of the swiss national forest inventory using
78 three-phase design-based regression estimation. Cana-
79 dian Journal of Forest Research 44(10):1177–1186, DOI
80 10.1139/cjfr-2014-0152, URL <https://doi.org/10.1139/cjfr-2014-0152>
- 81 Mathworks (2017) Matlab version 9.2.0.538062 (r2017a)
- 82 McRoberts RE, Tomppo EO, Næsset E (2010) Advances
83 and emerging issues in national forest inventories. Scan-
84 dinavian Journal of Forest Research 25(4):368–381,
85 DOI 10.1080/02827581.2010.496739, URL <http://dx.doi.org/10.1080/02827581.2010.496739>
- 86 McRoberts RE, Næsset E, Gobakken T, Bollandsås OM
87 (2015) Indirect and direct estimation of forest biomass
88 change using forest inventory and airborne laser scan-
89 ning data. Remote Sensing of Environment 164:36–
90 42, DOI 10.1016/j.rse.2015.02.018, URL <https://doi.org/10.1016/j.rse.2015.02.018>

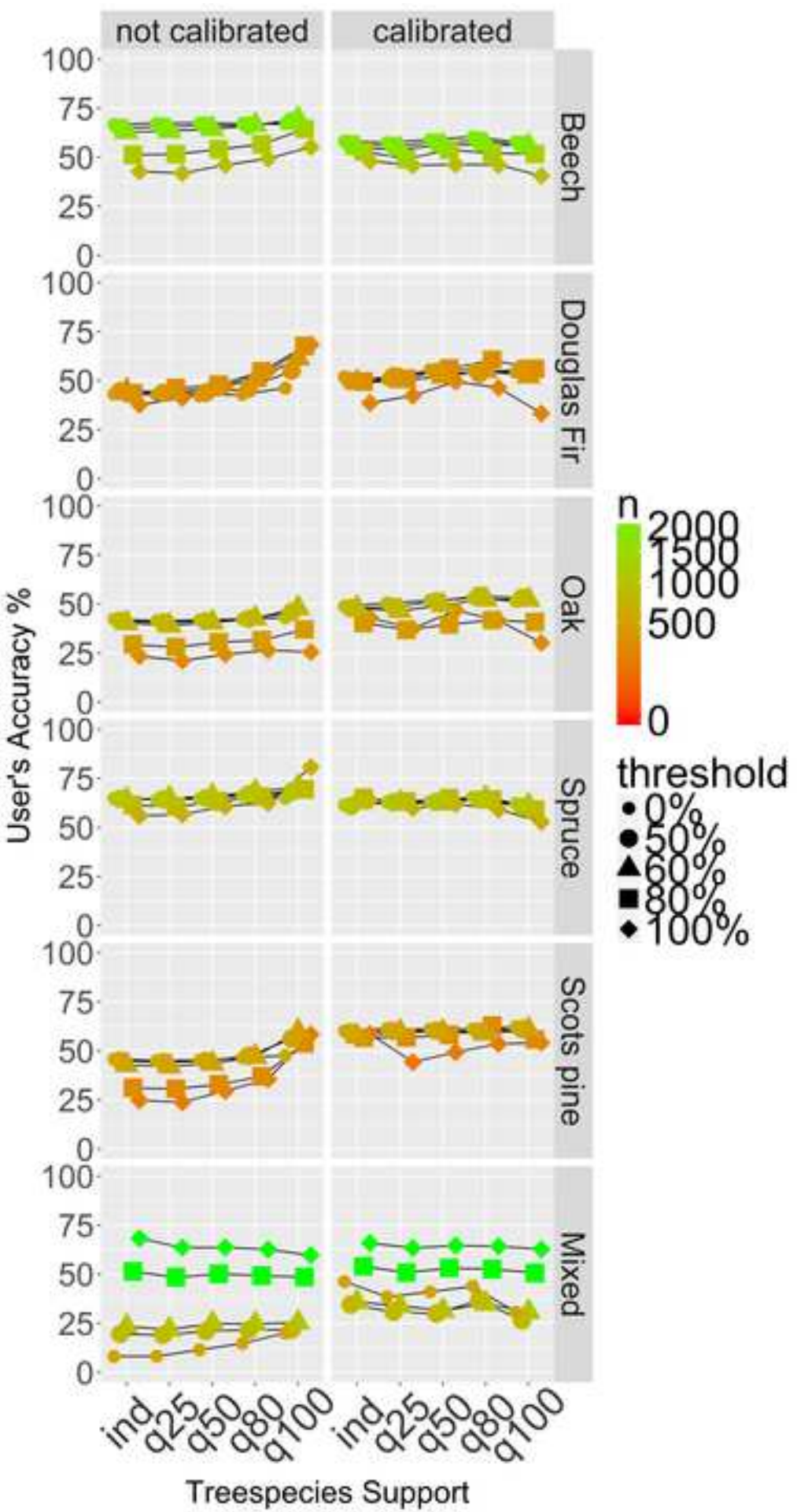
- 1 Naesset E (2014) Area-based inventory in norway – from
2 innovation to an operational reality. In: Forest Applications
3 of Airborne Laser Scanning - Concepts and Case
4 Studies, Springer, chap 11, pp 216–240, DOI 10.1007/
5 978-94-017-8663-8
- 6 Nink S, Hill J, Buddenbaum H, Stoffels J, Sachtleber T,
7 Langshausen J (2015) Assessing the suitability
8 of future multi-and hyperspectral satellite systems
9 for mapping the spatial distribution of norway spruce
10 timber volume. *Remote Sensing* 7(9):12,009–12,040,
11 DOI 10.3390/rs70912009, URL <http://www.mdpi.com/2072-4292/7/9/12009>
- 12 Packalén P, Maltamo M (2006) Predicting the plot volume
13 by tree species using airborne laser scanning and aerial
14 photographs. *Forest Science* 52(6):611–622
- 15 R Core Team (2016) R: A Language and Environment
16 for Statistical Computing. R Foundation for Statistical
17 Computing, Vienna, Austria, URL <https://www.R-project.org/>
- 18 Saborowski J, Marx A, Nagel J, Böckmann T (2010)
19 Double sampling for stratification in periodic inventories—
20 infinite population approach. *Forest ecology and management* 260(10):1886–1895, DOI 10.
21 1016/j.foreco.2010.08.035, URL <https://doi.org/10.1016/j.foreco.2010.08.035>
- 22 Schreuder HT, Gregoire TG, Wood GB (1993) Sampling
23 methods for multiresource forest inventory. John Wiley
24 & Sons
- 25 Stoffels J, Hill J, Sachtleber T, Mader S, Buddenbaum
26 H, Stern O, Langshausen J, Dietz J, Ontrup G (2015)
27 Satellite-based derivation of high-resolution forest information
28 layers for operational forest management. *Forests*
29 6(6):1982–2013, DOI 10.3390/f6061982, URL <http://www.mdpi.com/1999-4907/6/6/1982>
- 30 Straub C, Dees M, Weinacker H, Koch B (2009) Using air-
31 borne laser scanner data and cir orthophotos to estimate
32 the stem volume of forest stands. *Photogrammetrie-
33 Fernerkundung-Geoinformation* 2009(3):277–
34 287, DOI 10.1127/0935-1221/2009/0022, URL
35 <https://doi.org/10.1127/0935-1221/2009/0022>
- 36 von Thünen-Institut (2014) Dritte Bundeswaldinventur
37 2012. URL <https://bwi.info>, accessed: 2017-02-03
- 38 Tonolli S, Dalponte M, Vescovo L, Rodeghiero M, Bruzzone
39 L, Gianelle D (2011) Mapping and modeling forest tree
40 volume using forest inventory and airborne laser scanning.
41 *European Journal of Forest Research* 130(4):569–
42 577, DOI 10.1007/s10342-010-0445-5, URL <http://dx.doi.org/10.1007/s10342-010-0445-5>
- 43 Ullah S, Dees M, Datta P, Adler P, Koch B (2017) Comparing
44 airborne laser scanning, and image-based point clouds
45 by semi-global matching and enhanced automatic terrain
46 extraction to estimate forest timber volume. *Forests*
47 8(6):215, DOI 10.3390/f8060215, URL <http://www.mdpi.com/1999-4907/8/6/215>
- 48 Van Aardt J, Wynne R, Scrivani J (2008) Lidar-based map-
49 ping of forest volume and biomass by taxonomic group
50 using structurally homogenous segments. *Photogrammet-
51 ric Engineering & Remote Sensing* 74(8):1033–1044,
52 DOI 10.14358/PERS.74.8.1033, URL <https://doi.org/10.14358/PERS.74.8.1033>
- 53 White JC, Coops NC, Wulder MA, Vastaranta M, Hilker
54 T, Tompalski P (2016) Remote sensing technologies for
55 enhancing forest inventories: A review. *Canadian Journal
56 of Remote Sensing* 42(5):619–641, DOI 10.1080/
57 07038992.2016.1207484, URL <http://dx.doi.org/10.1080/07038992.2016.1207484>
- 58 Zianis D, Muukkonen P, Mäkipää R, Mencuccini M, et al
59 (2005) Biomass and stem volume equations for tree
60 species in Europe. *Silva Fennica Monographs* 4

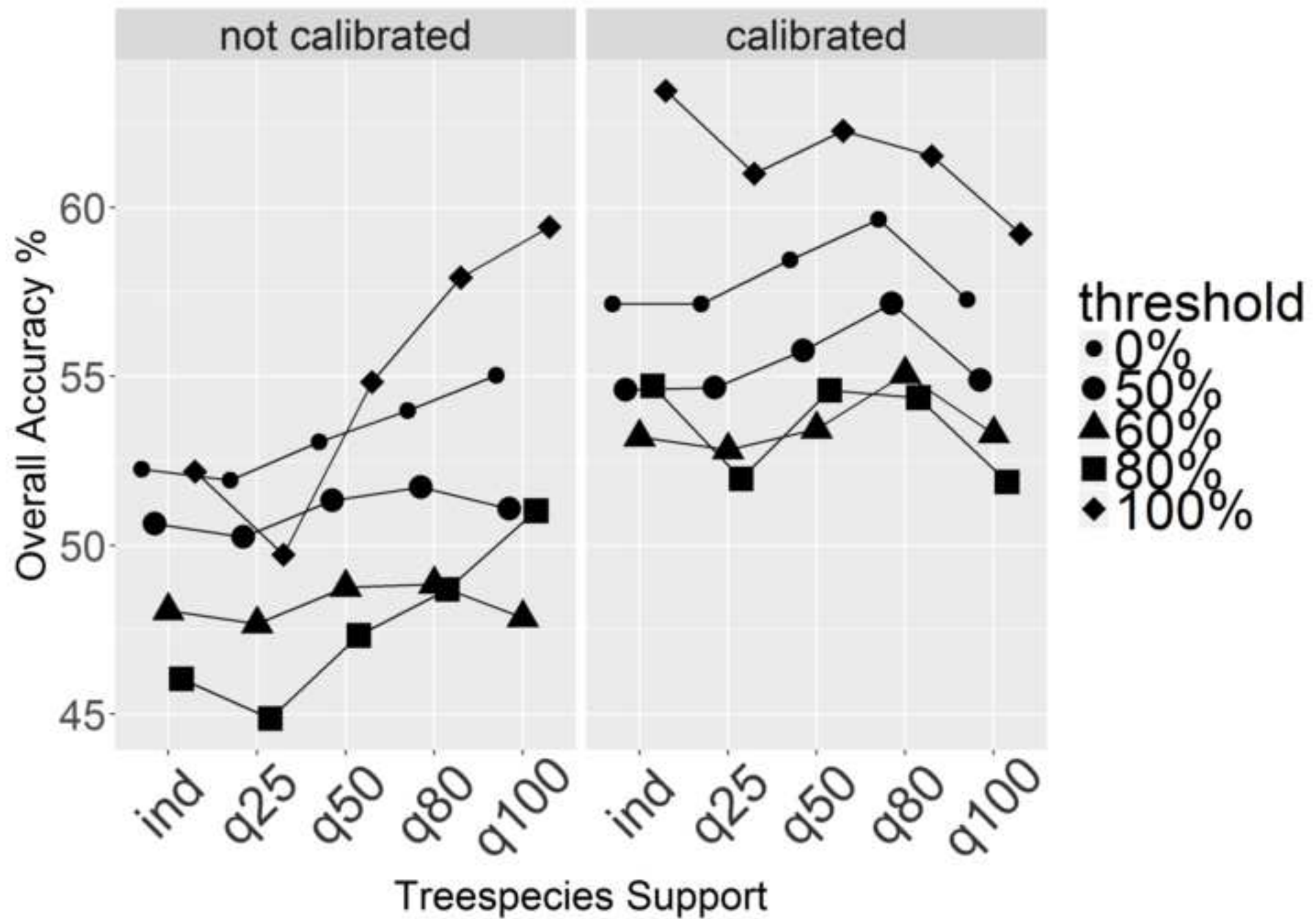


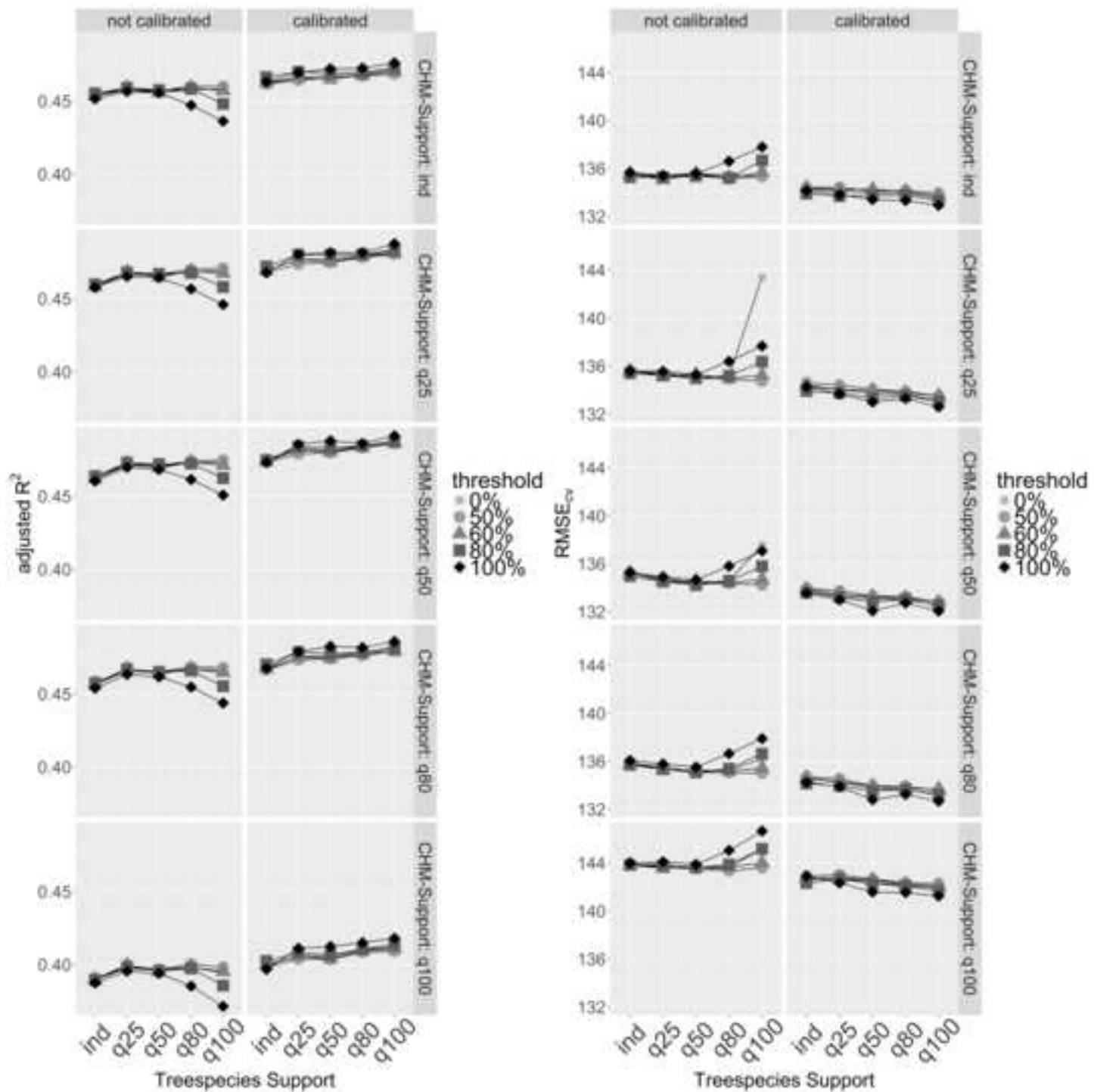


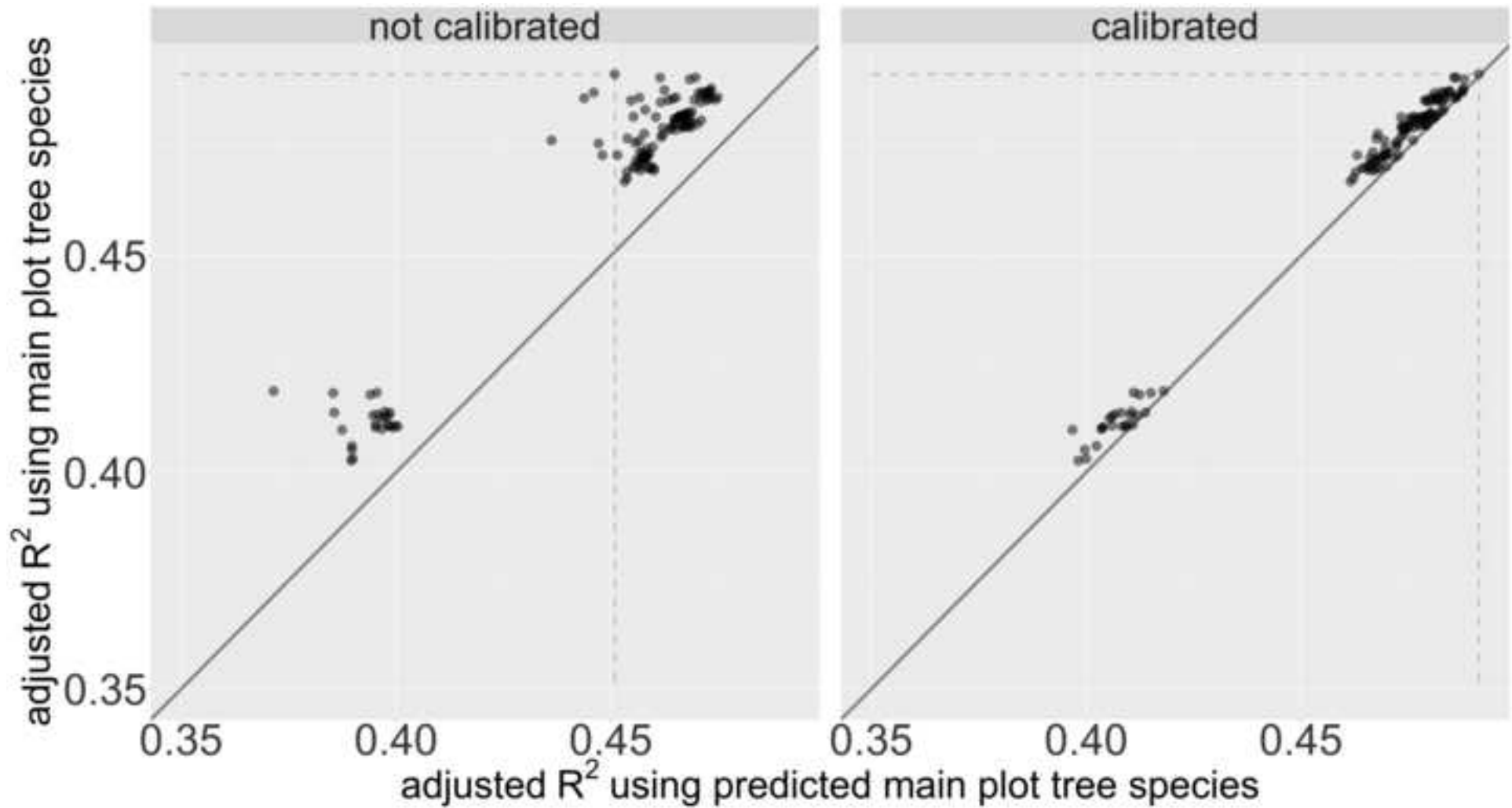


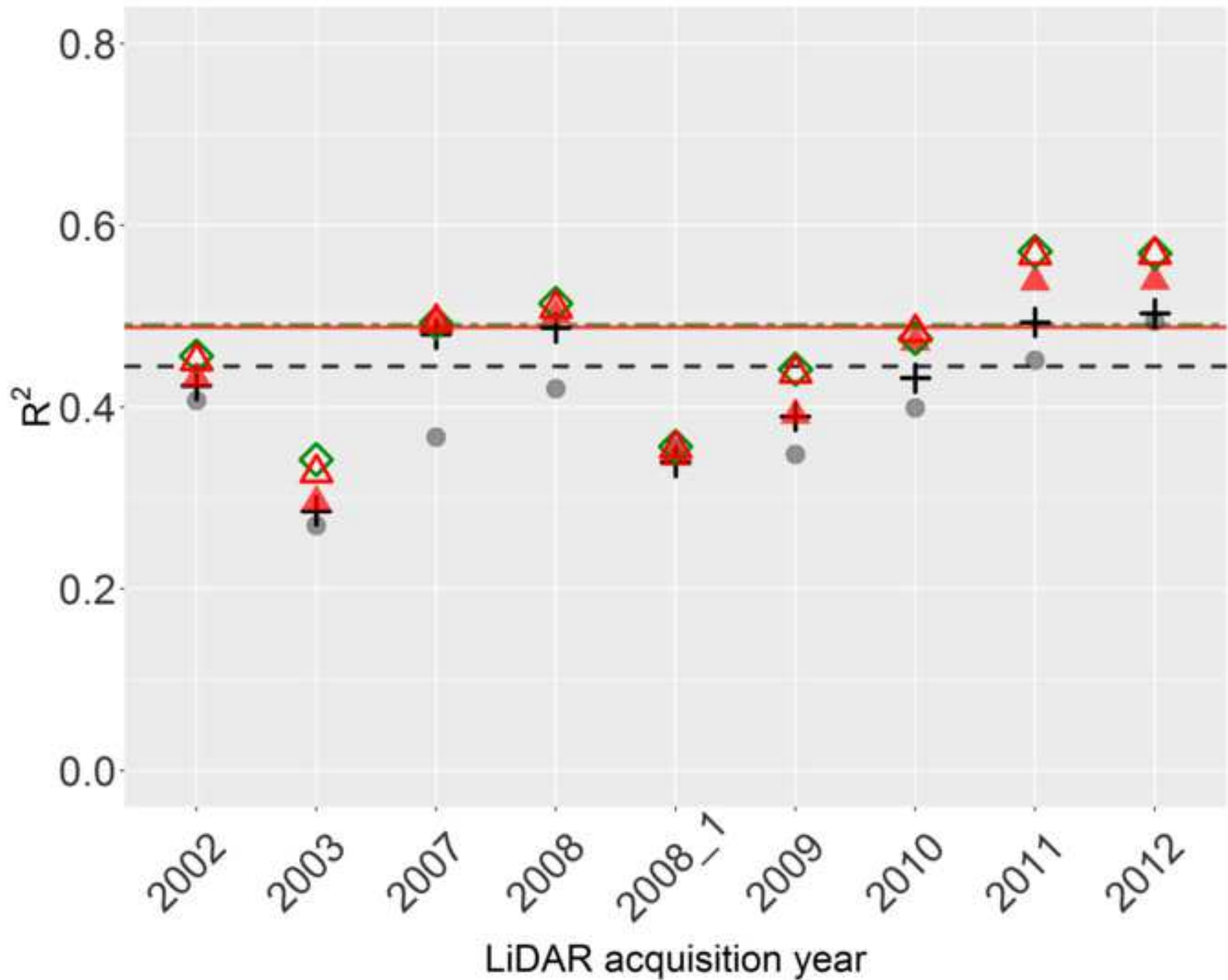


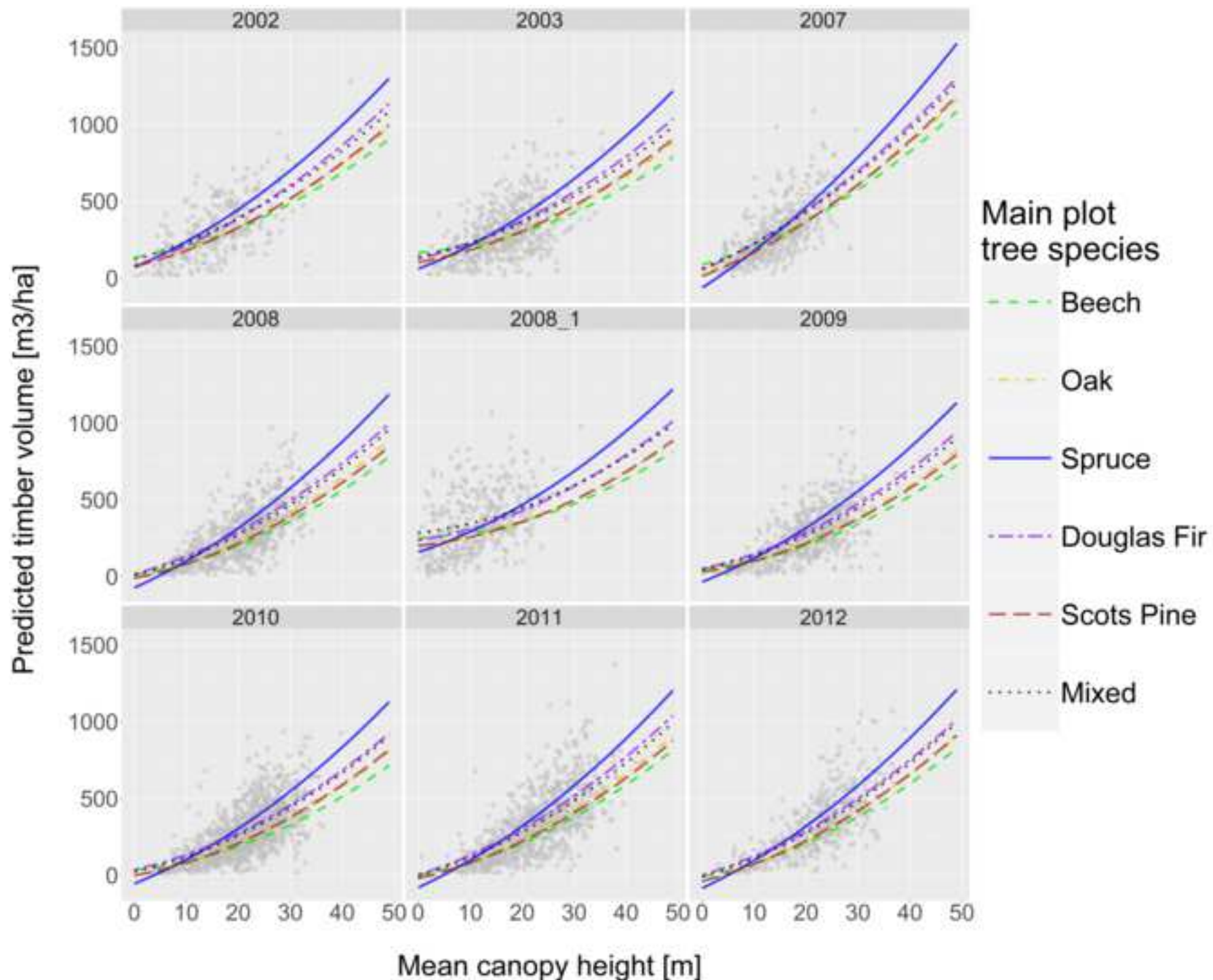












European Journal of Forest Research
Supplementary Material

**Combining canopy height and tree species
information for large scale timber volume
estimations under strong heterogeneity of
auxiliary data and variable sample plot sizes**

Andreas Hill*, Henning Buddenbaum , Daniel Mandallaz

* Corresponding author: andreas.hill@usys.ethz.ch

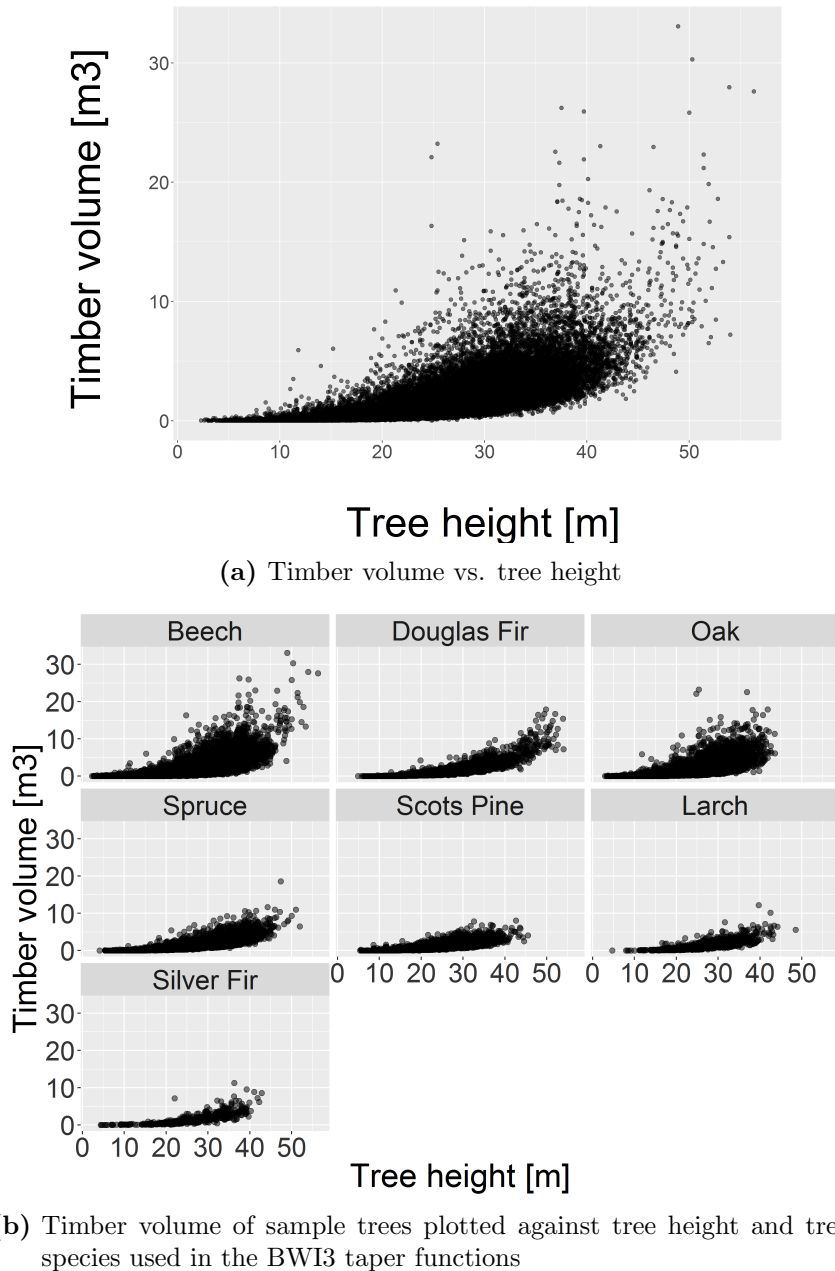
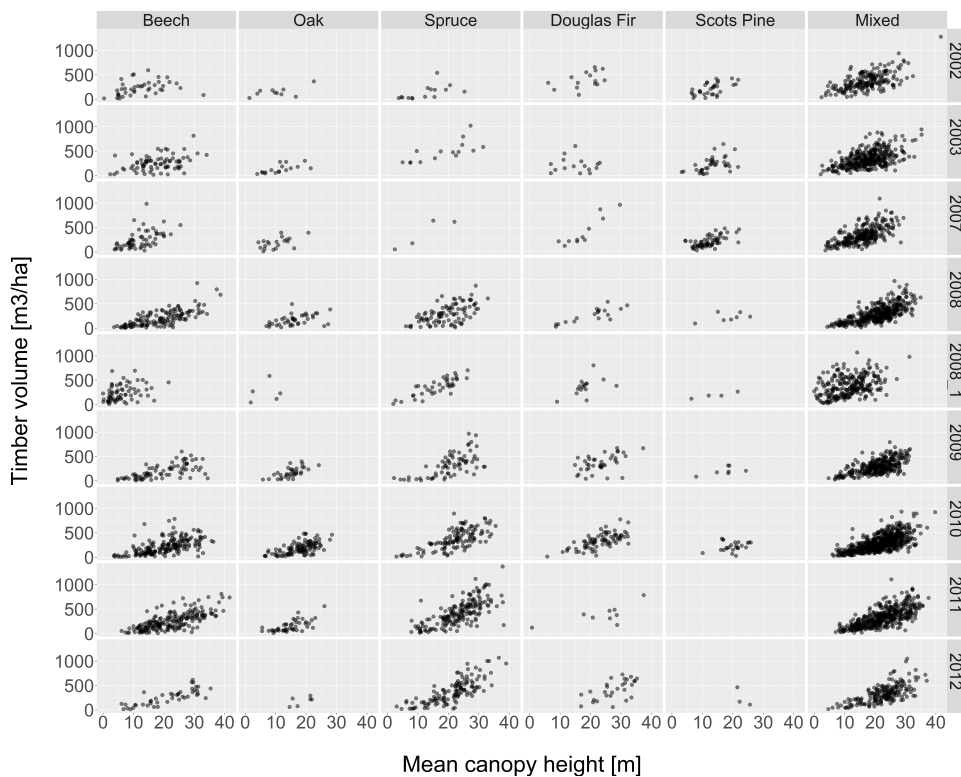
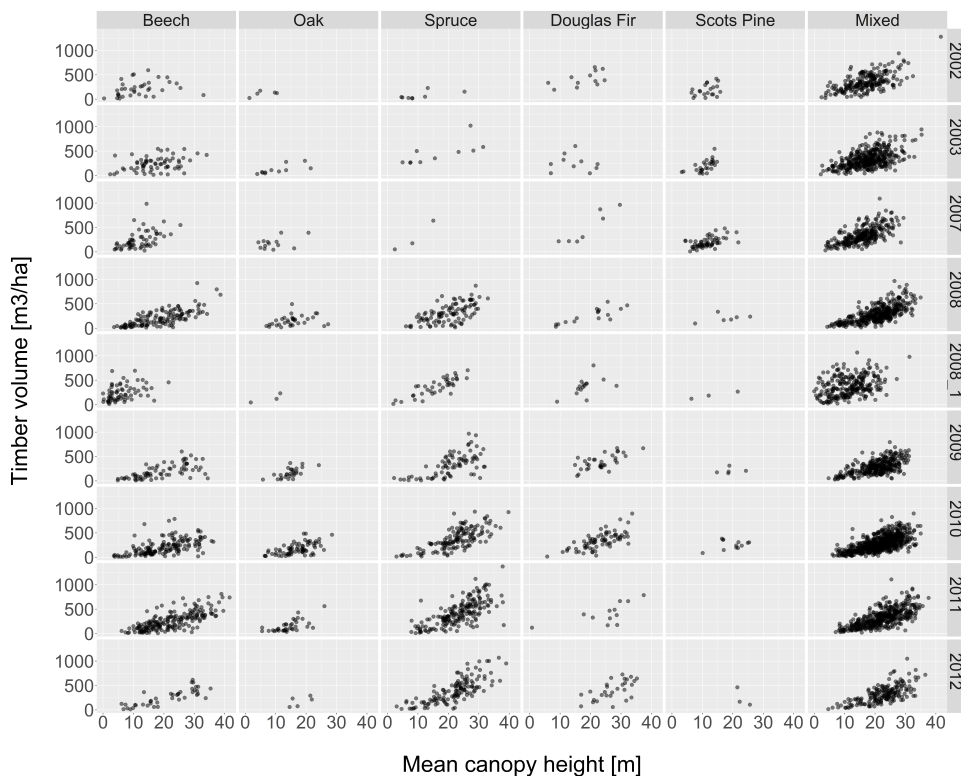
1: Timber volume - height relationship on single tree level

Figure 1: Timber volume relationships on single tree level of all BWI3 sample trees within RLP

2: Timber volume on plot level vs. predictor variables



(a) Timber volume on plot level vs. LiDAR *meanheight* stratified by the error-free *treespecies* variable



(b) Timber volume on plot level vs. LiDAR *meanheight* stratified by calibrated *treespecies* variable

Figure 2: Timber volume on sample plot level stratified by the *lidaryears* and *treespecies*

3: Classification accuracies of *treespecies* variable

Table 1: User's accuracies realized under various support choices for deriving the major tree species of a sample location. *class*: major tree species class of sample plot, *prod.acc*: producer's accuracy, *use.acc*: user's accuracy, *oaa*: overall accuracy, *prod.acc_{cal}*: producer's accuracy after calibration (*use.acc* and *oaa* respectively), *n.ref*: number of validation data per tree species.

class	support	threshold	prod.acc	prod.acc _{cal}	use.acc	use.acc _{cal}	oaa	oaa _{cal}	n.ref
Beech	ind	0%	50.77	70.64	66.69	58.31	52.25	57.14	1873
Douglas Fir	ind	0%	53.63	41.60	43.23	51.88	52.25	57.14	399
Oak	ind	0%	65.84	41.87	42.30	48.96	52.25	57.14	843
Spruce	ind	0%	58.60	68.88	64.89	61.55	52.25	57.14	1041
Scots pine	ind	0%	69.08	62.18	45.82	60.16	52.25	57.14	595
Mixed	ind	0%	3.23	16.51	8.17	46.28	52.25	57.14	527
Beech	ind	50%	50.95	69.24	65.00	56.82	50.63	54.60	1739
Douglas Fir	ind	50%	55.35	45.72	44.52	49.85	50.63	54.60	374
Oak	ind	50%	66.79	43.40	41.52	47.92	50.63	54.60	795
Spruce	ind	50%	58.84	69.28	64.54	60.90	50.63	54.60	996
Scots pine	ind	50%	69.34	60.77	45.13	59.46	50.63	54.60	548
Mixed	ind	50%	9.93	16.83	19.48	34.49	50.63	54.60	826
Beech	ind	60%	48.63	69.64	62.97	54.67	48.07	53.20	1647
Douglas Fir	ind	60%	53.44	44.90	45.01	49.10	48.07	53.20	363
Oak	ind	60%	64.44	42.51	40.33	47.89	48.07	53.20	748
Spruce	ind	60%	57.56	69.57	64.28	62.75	48.07	53.20	966
Scots pine	ind	60%	67.07	58.94	42.86	57.43	48.07	53.20	492
Mixed	ind	60%	16.38	20.53	23.36	35.86	48.07	53.20	1062
Beech	ind	80%	42.95	38.36	51.26	52.92	46.04	54.72	1134
Douglas Fir	ind	80%	46.00	37.33	43.53	49.56	46.04	54.72	300
Oak	ind	80%	64.19	21.86	29.36	40.34	46.04	54.72	430
Spruce	ind	80%	52.78	61.36	61.38	65.06	46.04	54.72	792
Scots pine	ind	80%	64.75	43.88	31.09	56.74	46.04	54.72	278
Mixed	ind	80%	39.72	69.92	51.41	54.00	46.04	54.72	2344
Beech	ind	100%	37.42	18.29	42.78	48.10	52.18	63.45	831
Douglas Fir	ind	100%	42.98	22.37	37.69	38.64	52.18	63.45	228
Oak	ind	100%	61.09	13.45	23.43	43.02	52.18	63.45	275
Spruce	ind	100%	49.38	52.66	55.93	63.83	52.18	63.45	640
Scots pine	ind	100%	62.01	28.49	24.78	58.62	52.18	63.45	179
Mixed	ind	100%	56.00	87.07	68.33	65.90	52.18	63.45	3125
Beech	q25	0%	50.18	72.59	67.44	57.54	51.92	57.14	1923
Douglas Fir	q25	0%	54.61	43.39	42.77	50.73	51.92	57.14	401
Oak	q25	0%	65.23	39.91	41.59	50.52	51.92	57.14	857
Spruce	q25	0%	58.71	68.79	64.07	62.71	51.92	57.14	1051
Scots pine	q25	0%	68.52	60.94	44.97	61.46	51.92	57.14	594
Mixed	q25	0%	3.17	12.50	8.21	38.51	51.92	57.14	536
Beech	q25	50%	50.67	71.31	65.56	55.85	50.24	54.66	1788
Douglas Fir	q25	50%	55.05	46.54	43.58	52.24	50.24	54.66	376
Oak	q25	50%	65.64	39.93	40.60	48.57	50.24	54.66	809
Spruce	q25	50%	59.05	69.48	64.36	62.86	50.24	54.66	1006
Scots pine	q25	50%	68.56	60.33	44.22	60.11	50.24	54.66	547
Mixed	q25	50%	9.69	15.43	19.01	30.86	50.24	54.66	836
Beech	q25	60%	48.32	70.89	63.37	54.12	47.67	52.82	1697
Douglas Fir	q25	60%	52.60	45.48	43.94	49.85	47.67	52.82	365
Oak	q25	60%	64.04	39.50	39.10	46.52	47.67	52.82	762
Spruce	q25	60%	58.20	69.36	64.91	62.51	47.67	52.82	976
Scots pine	q25	60%	67.21	56.82	42.09	59.62	47.67	52.82	491
Mixed	q25	60%	14.75	19.23	21.82	33.88	47.67	52.82	1071
Beech	q25	80%	42.27	38.80	51.55	49.14	44.87	51.96	1183
Douglas Fir	q25	80%	45.36	35.10	46.13	50.96	44.87	51.96	302
Oak	q25	80%	61.09	20.59	28.01	36.84	44.87	51.96	442
Spruce	q25	80%	52.43	62.55	60.69	63.26	44.87	51.96	801
Scots pine	q25	80%	63.67	38.85	30.62	56.84	44.87	51.96	278
Mixed	q25	80%	38.29	64.56	48.47	50.85	44.87	51.96	2356
Beech	q25	100%	35.27	15.93	41.89	45.90	49.72	61.00	879
Douglas Fir	q25	100%	40.43	21.74	41.15	42.37	49.72	61.00	230
Oak	q25	100%	54.36	7.32	21.08	37.50	49.72	61.00	287
Spruce	q25	100%	49.77	52.85	56.67	59.86	49.72	61.00	649
Scots pine	q25	100%	59.78	19.55	23.83	44.30	49.72	61.00	179
Mixed	q25	100%	53.44	85.47	63.59	63.39	49.72	61.00	3138

Continued on next page

class	support	threshold	prod.acc	<i>prod.acc_{cal}</i>	use.acc	<i>use.acc_{cal}</i>	oaa	<i>oaa_{cal}</i>	n.ref
Beech	q50	0%	51.14	73.60	67.53	59.03	53.06	58.45	1932
Douglas Fir	q50	0%	54.59	45.16	42.23	55.49	53.06	58.45	403
Oak	q50	0%	68.29	41.93	41.79	51.94	53.06	58.45	861
Spruce	q50	0%	59.92	70.47	64.65	63.26	53.06	58.45	1053
Scots pine	q50	0%	70.59	61.68	45.16	61.06	53.06	58.45	595
Mixed	q50	0%	1.85	13.52	11.49	41.01	53.06	58.45	540
Beech	q50	50%	51.64	72.06	66.10	57.58	51.32	55.76	1797
Douglas Fir	q50	50%	56.08	47.62	43.80	54.38	51.32	55.76	378
Oak	q50	50%	68.39	44.90	41.31	51.41	51.32	55.76	813
Spruce	q50	50%	60.22	69.74	64.92	63.05	51.32	55.76	1008
Scots pine	q50	50%	70.26	60.22	44.87	60.22	51.32	55.76	548
Mixed	q50	50%	8.93	15.36	21.01	29.93	51.32	55.76	840
Beech	q50	60%	48.21	70.26	64.42	56.17	48.76	53.44	1705
Douglas Fir	q50	60%	52.86	43.60	46.08	52.12	48.76	53.44	367
Oak	q50	60%	64.75	45.17	40.66	49.50	48.76	53.44	766
Spruce	q50	60%	58.69	69.73	65.98	62.34	48.76	53.44	978
Scots pine	q50	60%	67.07	55.28	43.54	59.65	48.76	53.44	492
Mixed	q50	60%	19.42	20.35	24.91	31.51	48.76	53.44	1076
Beech	q50	80%	41.21	44.91	54.08	53.78	47.33	54.59	1189
Douglas Fir	q50	80%	44.41	37.50	47.87	56.16	47.33	54.59	304
Oak	q50	80%	61.88	24.89	30.53	39.64	47.33	54.59	446
Spruce	q50	80%	52.30	63.76	63.35	64.81	47.33	54.59	803
Scots pine	q50	80%	63.67	39.57	32.90	58.20	47.33	54.59	278
Mixed	q50	80%	44.42	65.91	50.22	53.19	47.33	54.59	2364
Beech	q50	100%	29.56	20.16	46.11	46.35	54.83	62.26	883
Douglas Fir	q50	100%	33.04	23.91	47.50	49.55	54.83	62.26	230
Oak	q50	100%	47.75	10.38	24.34	46.88	54.83	62.26	289
Spruce	q50	100%	43.63	56.99	60.81	61.94	54.83	62.26	651
Scots pine	q50	100%	55.87	20.67	29.59	49.33	54.83	62.26	179
Mixed	q50	100%	66.40	85.06	63.69	64.59	54.83	62.26	3152
Beech	q80	0%	51.91	73.58	67.25	60.45	53.98	59.64	1938
Douglas Fir	q80	0%	55.91	47.04	42.99	55.52	53.98	59.64	406
Oak	q80	0%	68.55	46.82	42.30	53.01	53.98	59.64	865
Spruce	q80	0%	61.90	69.67	66.03	65.51	53.98	59.64	1055
Scots pine	q80	0%	71.74	64.21	46.48	61.15	53.98	59.64	598
Mixed	q80	0%	1.84	15.26	14.71	43.92	53.98	59.64	544
Beech	q80	50%	50.69	72.49	66.18	58.37	51.72	57.16	1803
Douglas Fir	q80	50%	54.86	45.67	46.04	53.54	51.72	57.16	381
Oak	q80	50%	67.93	48.84	42.43	54.21	51.72	57.16	817
Spruce	q80	50%	60.79	71.19	66.81	64.14	51.72	57.16	1010
Scots pine	q80	50%	71.58	61.02	47.41	59.71	51.72	57.16	549
Mixed	q80	50%	13.12	18.44	21.55	36.79	51.72	57.16	846
Beech	q80	60%	46.05	71.07	66.39	56.51	48.85	55.07	1711
Douglas Fir	q80	60%	49.73	47.30	50.41	55.03	48.85	55.07	370
Oak	q80	60%	63.90	48.18	42.75	52.33	48.85	55.07	770
Spruce	q80	60%	56.53	70.41	68.23	64.97	48.85	55.07	980
Scots pine	q80	60%	66.73	58.62	47.07	58.86	48.85	55.07	493
Mixed	q80	60%	27.17	21.81	24.66	35.01	48.85	55.07	1082
Beech	q80	80%	36.77	40.37	56.65	52.05	48.69	54.37	1194
Douglas Fir	q80	80%	39.74	37.46	54.71	60.53	48.69	54.37	307
Oak	q80	80%	56.47	24.55	31.59	41.83	48.69	54.37	448
Spruce	q80	80%	48.51	64.43	65.66	64.19	48.69	54.37	804
Scots pine	q80	80%	60.57	43.73	36.98	62.89	48.69	54.37	279
Mixed	q80	80%	53.03	67.06	49.26	52.61	48.69	54.37	2374
Beech	q80	100%	21.56	20.32	49.35	46.15	57.92	61.52	886
Douglas Fir	q80	100%	25.54	22.51	55.14	46.43	57.92	61.52	231
Oak	q80	100%	34.48	12.76	26.46	41.57	57.92	61.52	290
Spruce	q80	100%	32.36	50.46	62.61	59.17	57.92	61.52	652
Scots pine	q80	100%	44.44	25.00	35.56	53.57	57.92	61.52	180
Mixed	q80	100%	78.62	84.72	62.69	64.26	57.92	61.52	3167
Beech	q100	0%	53.72	70.93	66.92	57.90	55.03	57.27	1947
Douglas Fir	q100	0%	54.77	46.94	46.28	54.24	55.03	57.27	409
Oak	q100	0%	70.92	45.75	43.06	51.49	55.03	57.27	870
Spruce	q100	0%	62.30	66.07	64.87	62.20	55.03	57.27	1061
Scots pine	q100	0%	73.88	64.89	47.64	62.30	55.03	57.27	601
Mixed	q100	0%	0.36	9.76	20.00	30.68	55.03	57.27	553
Beech	q100	50%	46.96	69.43	68.35	56.39	51.08	54.88	1812
Douglas Fir	q100	50%	48.30	49.35	55.06	56.08	51.08	54.88	383
Oak	q100	50%	66.42	47.20	45.92	53.08	51.08	54.88	822
Spruce	q100	50%	56.00	67.42	68.14	60.67	51.08	54.88	1016

Continued on next page

class	support	threshold	prod.acc	<i>prod.acc_{cal}</i>	use.acc	<i>use.acc_{cal}</i>	oaa	<i>oaa_{cal}</i>	n.ref
Scots pine	q100	50%	67.57	63.22	56.26	61.12	51.08	54.88	552
Mixed	q100	50%	29.79	13.67	21.74	26.47	51.08	54.88	856
Beech	q100	60%	39.48	69.30	69.50	55.86	47.86	53.30	1720
Douglas Fir	q100	60%	39.78	44.35	61.41	52.22	47.86	53.30	372
Oak	q100	60%	58.45	46.84	47.99	52.23	47.86	53.30	775
Spruce	q100	60%	49.49	66.33	70.62	61.29	47.86	53.30	986
Scots pine	q100	60%	62.50	60.08	59.96	60.82	47.86	53.30	496
Mixed	q100	60%	48.17	20.88	25.40	30.85	47.86	53.30	1092
Beech	q100	80%	25.92	40.67	64.39	51.64	51.02	51.87	1200
Douglas Fir	q100	80%	23.62	27.18	67.59	56.00	51.02	51.87	309
Oak	q100	80%	44.15	24.06	37.04	40.82	51.02	51.87	453
Spruce	q100	80%	33.95	56.01	69.54	59.01	51.02	51.87	807
Scots pine	q100	80%	55.36	42.86	53.82	55.81	51.02	51.87	280
Mixed	q100	80%	73.70	65.59	48.59	50.65	51.02	51.87	2392
Beech	q100	100%	4.15	17.51	55.22	40.52	59.42	59.22	891
Douglas Fir	q100	100%	5.60	8.62	68.42	33.33	59.42	59.22	232
Oak	q100	100%	8.19	8.87	25.53	30.23	59.42	59.22	293
Spruce	q100	100%	10.28	41.26	80.72	52.75	59.42	59.22	652
Scots pine	q100	100%	20.99	28.73	58.46	54.17	59.42	59.22	181
Mixed	q100	100%	95.68	84.56	59.73	62.71	59.42	59.22	3192

4: Model accuracies

Table 2: Model accuracies realized under various support choices for the CHM- and **uncalibrated treespecies** explanatory variables

$support_{chm}$	$support_{t,spec}$	threshold	R^2_{adj}	$rmse_{cv}$	AIC	$R^2_{adj,ref}$	$rmse_{cv,ref}$	AIC_{ref}
ind	ind	0%	0.45	135.49	64565.00	0.47	133.56	64565.00
ind	ind	50%	0.45	135.57	64569.96	0.47	133.80	64569.96
ind	ind	60%	0.45	135.52	64564.50	0.47	133.73	64564.50
ind	ind	80%	0.46	135.26	64551.18	0.47	133.44	64551.18
ind	ind	100%	0.45	135.65	64584.58	0.47	133.03	64584.58
ind	q25	0%	0.46	135.37	64912.94	0.47	133.46	64912.94
ind	q25	50%	0.46	135.22	64899.31	0.47	133.81	64899.31
ind	q25	60%	0.46	135.07	64895.72	0.47	133.85	64895.72
ind	q25	80%	0.46	135.27	64896.97	0.47	133.36	64896.97
ind	q25	100%	0.46	135.42	64920.27	0.48	133.02	64920.27
ind	q50	0%	0.46	135.54	65166.10	0.47	133.61	65166.10
ind	q50	50%	0.46	135.52	65157.65	0.47	133.79	65157.65
ind	q50	60%	0.46	135.54	65168.94	0.47	133.68	65168.94
ind	q50	80%	0.46	135.35	65150.63	0.47	133.32	65150.63
ind	q50	100%	0.46	135.57	65168.81	0.48	132.93	65168.81
ind	q80	0%	0.46	135.44	65389.21	0.47	133.50	65389.21
ind	q80	50%	0.46	135.13	65367.67	0.47	133.87	65367.67
ind	q80	60%	0.46	135.21	65376.26	0.47	133.87	65376.26
ind	q80	80%	0.46	135.21	65384.06	0.47	133.44	65384.06
ind	q80	100%	0.45	136.59	65489.16	0.48	132.98	65489.16
ind	q100	0%	0.46	135.32	65722.46	0.47	133.45	65722.46
ind	q100	50%	0.46	135.32	65699.46	0.47	133.75	65699.46
ind	q100	60%	0.46	135.67	65728.34	0.47	133.69	65728.34
ind	q100	80%	0.45	136.66	65813.95	0.47	133.32	65813.95
ind	q100	100%	0.44	137.78	65919.21	0.48	132.91	65919.21
q25	ind	0%	0.46	135.53	64882.32	0.47	133.73	64882.32
q25	ind	50%	0.46	135.63	64886.16	0.47	134.07	64886.16
q25	ind	60%	0.46	135.58	64881.59	0.47	134.02	64881.59
q25	ind	80%	0.46	135.40	64869.18	0.48	133.58	64869.18
q25	ind	100%	0.46	135.58	64888.87	0.48	133.13	64888.87
q25	q25	0%	0.47	135.42	65600.99	0.48	133.37	65600.99
q25	q25	50%	0.47	135.24	65590.23	0.48	133.76	65590.23
q25	q25	60%	0.47	135.20	65586.93	0.48	133.71	65586.93
q25	q25	80%	0.47	135.21	65589.23	0.48	133.39	65589.23
q25	q25	100%	0.47	135.55	65616.63	0.49	132.97	65616.63
q25	q50	0%	0.47	135.02	65848.23	0.48	133.19	65848.23
q25	q50	50%	0.47	135.00	65842.32	0.48	133.40	65842.32
q25	q50	60%	0.46	135.28	65860.37	0.48	133.31	65860.37
q25	q50	80%	0.47	134.98	65839.14	0.48	133.00	65839.14
q25	q50	100%	0.46	135.27	65864.46	0.49	132.40	65864.46
q25	q80	0%	0.47	135.20	66065.23	0.48	133.26	66065.23
q25	q80	50%	0.47	134.93	66048.51	0.48	133.55	66048.51
q25	q80	60%	0.47	134.98	66059.78	0.48	133.53	66059.78
q25	q80	80%	0.47	135.19	66072.89	0.48	133.18	66072.89
q25	q80	100%	0.46	136.38	66178.69	0.49	132.75	66178.69
q25	q100	0%	0.47	143.40	66410.21	0.48	133.13	66410.21
q25	q100	50%	0.47	134.73	66384.24	0.48	133.39	66384.24
q25	q100	60%	0.47	135.23	66419.67	0.48	133.41	66419.67
q25	q100	80%	0.46	136.36	66511.85	0.48	133.01	66511.85
q25	q100	100%	0.45	137.67	66621.81	0.49	132.58	66621.81
q50	ind	0%	0.46	135.13	64847.79	0.48	133.11	64847.79
q50	ind	50%	0.46	135.24	64851.64	0.48	133.44	64851.64
q50	ind	60%	0.46	135.22	64847.03	0.48	133.43	64847.03
q50	ind	80%	0.46	134.96	64831.38	0.48	133.11	64831.38
q50	ind	100%	0.46	135.26	64862.89	0.48	132.62	64862.89
q50	q25	0%	0.47	134.80	65557.75	0.49	132.59	65557.75
q50	q25	50%	0.47	134.61	65546.50	0.49	132.92	65546.50
q50	q25	60%	0.47	134.57	65543.07	0.49	132.91	65543.07
q50	q25	80%	0.47	134.51	65540.80	0.49	132.69	65540.80
q50	q25	100%	0.47	134.92	65572.25	0.49	132.33	65572.25
q50	q50	0%	0.47	134.37	65805.45	0.49	132.36	65805.45
q50	q50	50%	0.47	134.34	65800.77	0.49	132.57	65800.77

Continued on next page

$support_{chm}$	$support_{t,spec}$	threshold	R^2_{adj}	$rmse_{cv}$	AIC	$R^2_{adj,ref}$	$rmse_{cv,ref}$	AIC_{ref}
q50	q50	60%	0.47	134.53	65815.15	0.49	132.54	65815.15
q50	q50	80%	0.47	134.21	65789.54	0.49	132.25	65789.54
q50	q50	100%	0.47	134.66	65825.59	0.49	131.74	65825.59
q50	q80	0%	0.47	134.57	66019.32	0.49	132.53	66019.32
q50	q80	50%	0.47	134.36	66006.32	0.49	132.82	66006.32
q50	q80	60%	0.47	134.41	66015.77	0.49	132.79	66015.77
q50	q80	80%	0.47	134.57	66025.39	0.49	132.62	66025.39
q50	q80	100%	0.46	135.80	66132.10	0.49	132.18	66132.10
q50	q100	0%	0.47	137.56	66365.96	0.49	132.48	66365.96
q50	q100	50%	0.47	134.21	66345.91	0.49	132.72	66345.91
q50	q100	60%	0.47	134.69	66381.21	0.49	132.72	66381.21
q50	q100	80%	0.46	135.78	66468.28	0.49	132.46	66468.28
q50	q100	100%	0.45	137.06	66575.44	0.49	132.03	66575.44
q80	ind	0%	0.46	135.78	64898.36	0.47	133.82	64898.36
q80	ind	50%	0.46	135.90	64900.98	0.47	134.21	64900.98
q80	ind	60%	0.46	135.85	64895.77	0.47	134.20	64895.77
q80	ind	80%	0.46	135.70	64890.76	0.47	133.79	64890.76
q80	ind	100%	0.45	136.06	64925.51	0.48	133.26	64925.51
q80	q25	0%	0.47	135.53	65611.68	0.48	133.44	65611.68
q80	q25	50%	0.47	135.36	65600.46	0.48	133.78	65600.46
q80	q25	60%	0.47	135.29	65595.97	0.48	133.76	65595.97
q80	q25	80%	0.47	135.35	65599.65	0.48	133.53	65599.65
q80	q25	100%	0.46	135.78	65634.33	0.49	133.04	65634.33
q80	q50	0%	0.46	135.09	65860.84	0.48	133.11	65860.84
q80	q50	50%	0.47	135.10	65857.40	0.48	133.40	65857.40
q80	q50	60%	0.46	135.25	65869.26	0.48	133.39	65869.26
q80	q50	80%	0.47	135.08	65857.71	0.48	133.06	65857.71
q80	q50	100%	0.46	135.52	65890.97	0.49	132.45	65890.97
q80	q80	0%	0.47	135.29	66078.42	0.48	133.27	66078.42
q80	q80	50%	0.47	135.06	66063.08	0.48	133.60	66063.08
q80	q80	60%	0.47	135.20	66077.30	0.48	133.60	66077.30
q80	q80	80%	0.47	135.38	66089.20	0.48	133.33	66089.20
q80	q80	100%	0.45	136.64	66197.34	0.49	132.82	66197.34
q80	q100	0%	0.47	136.20	66438.48	0.48	133.22	66438.48
q80	q100	50%	0.47	135.00	66413.28	0.48	133.51	66413.28
q80	q100	60%	0.46	135.43	66445.71	0.48	133.51	66445.71
q80	q100	80%	0.46	136.63	66538.24	0.48	133.16	66538.24
q80	q100	100%	0.44	137.89	66642.87	0.49	132.64	66642.87
q100	ind	0%	0.39	143.82	65494.94	0.41	142.07	65494.94
q100	ind	50%	0.39	143.93	65496.27	0.40	142.38	65496.27
q100	ind	60%	0.39	143.83	65492.62	0.40	142.41	65492.62
q100	ind	80%	0.39	143.83	65494.72	0.41	142.00	65494.72
q100	ind	100%	0.39	143.98	65512.77	0.41	141.55	65512.77
q100	q25	0%	0.40	143.88	66234.56	0.41	141.95	66234.56
q100	q25	50%	0.40	143.64	66219.68	0.41	142.27	66219.68
q100	q25	60%	0.40	143.56	66214.76	0.41	142.30	66214.76
q100	q25	80%	0.40	143.77	66225.18	0.41	141.99	66225.18
q100	q25	100%	0.40	144.09	66251.66	0.42	141.48	66251.66
q100	q50	0%	0.40	143.49	66484.62	0.41	141.65	66484.62
q100	q50	50%	0.40	143.52	66483.55	0.41	141.96	66483.55
q100	q50	60%	0.40	143.69	66495.93	0.41	141.97	66495.93
q100	q50	80%	0.40	143.62	66491.72	0.41	141.63	66491.72
q100	q50	100%	0.39	143.87	66506.91	0.42	140.99	66506.91
q100	q80	0%	0.40	143.60	66712.36	0.41	141.85	66712.36
q100	q80	50%	0.40	143.35	66693.16	0.41	142.18	66693.16
q100	q80	60%	0.40	143.66	66712.41	0.41	142.19	66712.41
q100	q80	80%	0.40	143.86	66719.35	0.41	141.86	66719.35
q100	q80	100%	0.39	145.04	66822.81	0.42	141.32	66822.81
q100	q100	0%	0.39	145.21	67092.26	0.41	142.01	67092.26
q100	q100	50%	0.40	143.61	67060.58	0.41	142.24	67060.58
q100	q100	60%	0.40	144.01	67086.87	0.41	142.25	67086.87
q100	q100	80%	0.39	145.17	67169.91	0.41	141.79	67169.91
q100	q100	100%	0.37	146.66	67284.45	0.42	141.22	67284.45

Table 3: Model accuracies realized under various support choices for the CHM- and **calibrated treespecies** explanatory variables

$support_{chm}$	$support_{t_{spec}}$	threshold	R^2_{adj}	$rmse_{cv}$	AIC	$R^2_{adj,ref}$	$rmse_{cv,ref}$	AIC_{ref}
ind	ind	0%	0.46	134.23	64480.01	0.47	133.56	64480.01
ind	ind	50%	0.46	134.42	64491.42	0.47	133.80	64491.42
ind	ind	60%	0.46	134.39	64485.07	0.47	133.73	64485.07
ind	ind	80%	0.47	133.90	64445.55	0.47	133.44	64445.55
ind	ind	100%	0.46	134.15	64476.36	0.47	133.03	64476.36
ind	q25	0%	0.47	134.16	64829.60	0.47	133.46	64829.60
ind	q25	50%	0.46	134.40	64847.07	0.47	133.81	64847.07
ind	q25	60%	0.47	134.24	64831.79	0.47	133.85	64831.79
ind	q25	80%	0.47	133.68	64791.42	0.47	133.36	64791.42
ind	q25	100%	0.47	133.81	64796.95	0.48	133.02	64796.95
ind	q50	0%	0.47	133.96	65056.48	0.47	133.61	65056.48
ind	q50	50%	0.47	134.14	65070.88	0.47	133.79	65070.88
ind	q50	60%	0.46	134.27	65080.88	0.47	133.68	65080.88
ind	q50	80%	0.47	133.75	65038.93	0.47	133.32	65038.93
ind	q50	100%	0.47	133.41	65011.19	0.48	132.93	65011.19
ind	q80	0%	0.47	133.95	65287.34	0.47	133.50	65287.34
ind	q80	50%	0.47	134.16	65300.34	0.47	133.87	65300.34
ind	q80	60%	0.47	134.08	65293.82	0.47	133.87	65293.82
ind	q80	80%	0.47	133.77	65275.66	0.47	133.44	65275.66
ind	q80	100%	0.47	133.32	65246.11	0.48	132.98	65246.11
ind	q100	0%	0.47	133.53	65586.83	0.47	133.45	65586.83
ind	q100	50%	0.47	133.94	65618.19	0.47	133.75	65618.19
ind	q100	60%	0.47	133.70	65603.53	0.47	133.69	65603.53
ind	q100	80%	0.47	133.32	65576.24	0.47	133.32	65576.24
ind	q100	100%	0.48	132.92	65542.94	0.48	132.91	65542.94
q25	ind	0%	0.47	134.41	64780.16	0.47	133.73	64780.16
q25	ind	50%	0.47	134.61	64794.59	0.47	134.07	64794.59
q25	ind	60%	0.47	134.33	64777.60	0.47	134.02	64777.60
q25	ind	80%	0.47	133.93	64756.34	0.48	133.58	64756.34
q25	ind	100%	0.47	134.29	64791.96	0.48	133.13	64791.96
q25	q25	0%	0.48	134.03	65504.85	0.48	133.37	65504.85
q25	q25	50%	0.47	134.42	65534.10	0.48	133.76	65534.10
q25	q25	60%	0.48	134.02	65502.59	0.48	133.71	65502.59
q25	q25	80%	0.48	133.76	65475.16	0.48	133.39	65475.16
q25	q25	100%	0.48	133.67	65467.58	0.49	132.97	65467.58
q25	q50	0%	0.48	133.77	65744.39	0.48	133.19	65744.39
q25	q50	50%	0.47	134.06	65767.28	0.48	133.40	65767.28
q25	q50	60%	0.48	133.98	65763.30	0.48	133.31	65763.30
q25	q50	80%	0.48	133.34	65715.59	0.48	133.00	65715.59
q25	q50	100%	0.48	133.00	65694.99	0.49	132.40	65694.99
q25	q80	0%	0.48	133.60	65960.24	0.48	133.26	65960.24
q25	q80	50%	0.48	133.87	65973.16	0.48	133.55	65973.16
q25	q80	60%	0.48	133.77	65963.19	0.48	133.53	65963.19
q25	q80	80%	0.48	133.52	65950.49	0.48	133.18	65950.49
q25	q80	100%	0.48	133.30	65934.08	0.49	132.75	65934.08
q25	q100	0%	0.48	133.18	66271.97	0.48	133.13	66271.97
q25	q100	50%	0.48	133.52	66295.64	0.48	133.39	66295.64
q25	q100	60%	0.48	133.52	66290.29	0.48	133.41	66290.29
q25	q100	80%	0.48	133.04	66266.45	0.48	133.01	66266.45
q25	q100	100%	0.49	132.59	66221.95	0.49	132.58	66221.95
q50	ind	0%	0.47	133.79	64739.35	0.48	133.11	64739.35
q50	ind	50%	0.47	133.95	64745.34	0.48	133.44	64745.34
q50	ind	60%	0.47	133.88	64738.45	0.48	133.43	64738.45
q50	ind	80%	0.47	133.58	64730.79	0.48	133.11	64730.79
q50	ind	100%	0.47	133.54	64739.74	0.48	132.62	64739.74
q50	q25	0%	0.48	133.26	65448.81	0.49	132.59	65448.81
q50	q25	50%	0.48	133.75	65481.44	0.49	132.92	65481.44
q50	q25	60%	0.48	133.43	65453.59	0.49	132.91	65453.59
q50	q25	80%	0.48	133.21	65432.13	0.49	132.69	65432.13
q50	q25	100%	0.49	132.99	65414.52	0.49	132.33	65414.52
q50	q50	0%	0.48	133.16	65703.73	0.49	132.36	65703.73
q50	q50	50%	0.48	133.31	65716.88	0.49	132.57	65716.88
q50	q50	60%	0.48	133.26	65712.36	0.49	132.54	65712.36
q50	q50	80%	0.48	132.81	65683.06	0.49	132.25	65683.06
q50	q50	100%	0.49	132.07	65629.14	0.49	131.74	65629.14

Continued on next page

$support_{chm}$	$support_{t,spec}$	threshold	R^2_{adj}	$rmse_{cv}$	AIC	$R^2_{adj,ref}$	$rmse_{cv,ref}$	AIC_{ref}
q50	q80	0%	0.48	132.97	65907.36	0.49	132.53	65907.36
q50	q80	50%	0.48	133.24	65921.57	0.49	132.82	65921.57
q50	q80	60%	0.48	133.13	65916.29	0.49	132.79	65916.29
q50	q80	80%	0.48	133.03	65908.22	0.49	132.62	65908.22
q50	q80	100%	0.49	132.72	65887.21	0.49	132.18	65887.21
q50	q100	0%	0.49	132.60	66219.82	0.49	132.48	66219.82
q50	q100	50%	0.49	132.78	66236.92	0.49	132.72	66236.92
q50	q100	60%	0.49	132.81	66234.74	0.49	132.72	66234.74
q50	q100	80%	0.49	132.55	66222.37	0.49	132.46	66222.37
q50	q100	100%	0.49	132.06	66177.66	0.49	132.03	66177.66
q80	ind	0%	0.47	134.57	64803.25	0.47	133.82	64803.25
q80	ind	50%	0.47	134.71	64807.20	0.47	134.21	64807.20
q80	ind	60%	0.47	134.60	64797.25	0.47	134.20	64797.25
q80	ind	80%	0.47	134.16	64773.29	0.47	133.79	64773.29
q80	ind	100%	0.47	134.25	64795.59	0.48	133.26	64795.59
q80	q25	0%	0.48	134.25	65515.53	0.48	133.44	65515.53
q80	q25	50%	0.47	134.54	65537.15	0.48	133.78	65537.15
q80	q25	60%	0.48	134.29	65517.64	0.48	133.76	65517.64
q80	q25	80%	0.48	133.94	65484.54	0.48	133.53	65484.54
q80	q25	100%	0.48	133.89	65481.53	0.49	133.04	65481.53
q80	q50	0%	0.48	133.76	65751.41	0.48	133.11	65751.41
q80	q50	50%	0.47	133.96	65768.65	0.48	133.40	65768.65
q80	q50	60%	0.47	133.95	65766.20	0.48	133.39	65766.20
q80	q50	80%	0.48	133.52	65734.51	0.48	133.06	65734.51
q80	q50	100%	0.48	132.80	65683.87	0.49	132.45	65683.87
q80	q80	0%	0.48	133.61	65964.09	0.48	133.27	65964.09
q80	q80	50%	0.48	133.91	65986.91	0.48	133.60	65986.91
q80	q80	60%	0.48	133.75	65973.94	0.48	133.60	65973.94
q80	q80	80%	0.48	133.65	65964.87	0.48	133.33	65964.87
q80	q80	100%	0.48	133.25	65931.80	0.49	132.82	65931.80
q80	q100	0%	0.48	133.29	66282.17	0.48	133.22	66282.17
q80	q100	50%	0.48	133.58	66307.14	0.48	133.51	66307.14
q80	q100	60%	0.48	133.69	66308.78	0.48	133.51	66308.78
q80	q100	80%	0.48	133.19	66281.98	0.48	133.16	66281.98
q80	q100	100%	0.49	132.68	66234.70	0.49	132.64	66234.70
q100	ind	0%	0.40	142.64	65410.22	0.41	142.07	65410.22
q100	ind	50%	0.40	142.88	65422.90	0.40	142.38	65422.90
q100	ind	60%	0.40	142.72	65407.17	0.40	142.41	65407.17
q100	ind	80%	0.40	142.34	65386.95	0.41	142.00	65386.95
q100	ind	100%	0.40	142.91	65434.69	0.41	141.55	65434.69
q100	q25	0%	0.41	142.73	66160.90	0.41	141.95	66160.90
q100	q25	50%	0.40	143.01	66179.74	0.41	142.27	66179.74
q100	q25	60%	0.41	142.73	66160.25	0.41	142.30	66160.25
q100	q25	80%	0.41	142.68	66141.80	0.41	141.99	66141.80
q100	q25	100%	0.41	142.34	66116.49	0.42	141.48	66116.49
q100	q50	0%	0.41	142.42	66407.67	0.41	141.65	66407.67
q100	q50	50%	0.40	142.65	66424.41	0.41	141.96	66424.41
q100	q50	60%	0.40	142.62	66421.19	0.41	141.97	66421.19
q100	q50	80%	0.41	142.29	66396.88	0.41	141.63	66396.88
q100	q50	100%	0.41	141.58	66346.14	0.42	140.99	66346.14
q100	q80	0%	0.41	142.10	66605.90	0.41	141.85	66605.90
q100	q80	50%	0.41	142.34	66622.90	0.41	142.18	66622.90
q100	q80	60%	0.41	142.23	66613.83	0.41	142.19	66613.83
q100	q80	80%	0.41	142.07	66603.97	0.41	141.86	66603.97
q100	q80	100%	0.42	141.53	66562.97	0.42	141.32	66562.97
q100	q100	0%	0.41	141.98	66941.24	0.41	142.01	66941.24
q100	q100	50%	0.41	142.27	66965.61	0.41	142.24	66965.61
q100	q100	60%	0.41	142.08	66949.79	0.41	142.25	66949.79
q100	q100	80%	0.41	141.67	66923.58	0.41	141.79	66923.58
q100	q100	100%	0.42	141.24	66885.59	0.42	141.22	66885.59